We get by with a little help from our friends: diversity begets diversity through shared adaptive genetic variation

Emilie J. Richards[1,2] and Christopher H. Martin[1,2]

[1]Department of Integrative Biology, University of California, Berkeley

[2]Museum of Vertebrate Zoology, University of California, Berkeley

Correspondence: *chmartin@berkeley.edu*

Keywords: ecological speciation, ecomorph, adaptive radiation, novelty, innovation, selective sweep

Abstract

Adaptive radiations involve astounding bursts of phenotypic, ecological, and species diversity. However, the microevolutionary processes that underlie the origins of these bursts are still poorly understood. We report the discovery of a cryptic 'wide-mouth' intermediate scale-eating ecomorph in a sympatric radiation of *Cyprinodon* pupfishes which provides crucial information about the evolutionary and ecological transition from a widespread algae-eating generalist to a novel microendemic scale-eating specialist. We first show that this ecomorph occurs in sympatry with generalist *C. variegatus* and scale-eating specialist *C. desquamator* across several hypersaline lakes on San Salvador Island, Bahamas, but is genetically differentiated, morphologically distinct when reared in a common garden, and sometimes consumes scales. We then compared the timing of selective sweeps on shared and unique adaptive variants in both scale-eating species to characterize the evolutionary path to scale-eating. We predicted that adaptation to the intermediate *C.* sp. 'wide-mouth' scale-eating niche aided in the rapid divergence of the more specialized scale-eater *C. desquamator*. Therefore, selection for shared adaptive variants should occur first in 'wide-mouth'. Contrary to our prediction, four of the six sets of shared adaptive alleles in both scale-eating species swept significantly earlier in *C. desquamator*. Adaptive introgression from *desquamator* into the 'wide-mouth' ancestor may have resulted in parallel evolution of their dietary niche. Conversely, no adaptive alleles for scale-eating were reused in a third sympatric molluscivore specialist *C. brontotheriodes*, despite sharing 9% of hard selective sweeps. Our work provides a microevolutionary framework for investigating how 'diversity begets diversity' during adaptive radiation.

Author Summary

Adaptive radiations present a paradox to our understanding of the mechanisms that drive speciation. The hallmark of adaptive radiation is a rapid, sustained burst of ecological, phenotypic, and species diversity yet many theoretical models predict that diversification should slow down with each event. Alternatively, radiations could be self-propagating and the diversity generated within the first stages of radiation could beget further diversity. The microevolutionary processes underlying this hypothesis are poorly understood. We propose that the exchange of adaptive alleles from one population could help other populations colonize new fitness peaks and promote further diversification across the fitness landscape. Here we explore the role of shared adaptive alleles in a recent radiation of trophic specialist pupfishes and characterize a cryptic new scale-eating species (*C. sp.* 'wide-mouth') through morphological, dietary, and genomic analyses. We discovered shared selective sweeps among all three specialists in this radiation despite their divergent morphologies and ecologies. We also found that adaptive introgression from the more specialized scale-eater *C. desquamator* may have provided access to a similar niche in the recently discovered intermediate scale-eater. Our findings of shared adaptive alleles and selective sweeps across multiple specialists within a radiation provide support for the hypothesis that diversity begets diversity and insight into the underlying microevolutionary process.

Introduction

Rapid bursts of diversification and repeated bouts of speciation like those seen in adaptive radiations contradict many of our existing mechanistic models for understanding speciation (reviewed in [1]). For example, many speciation models predict that diversification should slow with time as available niche space becomes increasingly subdivided and disruptive selection becomes weaker with each recurrent speciation event (e.g. [2–5]). Diversification on complex adaptive landscapes with multiple empty fitness peaks corresponding to different niches provides an alternative mechanism to niche subdivision and might better explain how a rapid burst of radiation can occur [6–9]. There is increasing empirical support for the complexity of fitness landscapes in nature [10–16] . However, these landscapes present a new problem: How do populations manage to escape local optima, cross fitness valleys, and access new fitness peaks [10–12,17–20]?

Colonizing new fitness peaks on the adaptive landscape often requires transitions in behaviors, morphological traits, or a combination of the two that allow organisms to adapt to new ecological niches [21]. Some of the most spectacular ecological transitions occur during adaptive radiations, such as blood-drinking [22] or plant carnivory [23,24]. Adaptation to novel fitness peaks is a hallmark of adaptive radiation, yet it is still poorly understood how such seemingly discontinuous transitions occur. An early hypothesis for how these transitions occurred was through ‘macromutational’ leaps that resulted in ‘hopeful monsters’ [25,26]. Although these ideas were eventually discounted by the insights of the Modern Synthesis [27–30], recent empirical and theoretical research on hybrid speciation has revived an appreciation for the rapid evolution of novelty through transgressive phenotypes resulting from hybridization. For example, hybridization between two species of sunflowers led to new hybrid species with suites of transgressive traits that allowed them to colonize novel sand dune and salt marsh

habitats [31,32]. However, the transgressive effects of hybridization are so myriad [33,34] that conditions for hybridization triggering the evolution of new species or new ecological niches are still poorly understood and contentious in diploid taxa [35,36].

Recent conceptual frameworks for understanding adaptation to novel fitness peaks suggest that ecological transitions are more likely to occur in stages [37–39]. The initial emergence of a novel trait is likely to require further adaptive refinement to become successfully incorporated into the functional ecology of an organism. One of the best examples is the evolution of the novel niche of aerobic citrate metabolism in *E. coli*, in which evolution of *citT* promotor capture in one intermediate lineage actualized the phenotype of aerobic citrate metabolism while further mutations at *dctA* in subsequent lineages refined the efficiency of citrate utilization that allowed it to fully occupy this niche [39–42]. This important set of studies suggests that novel ecological transitions are highly contingent on a complex series of mutations that potentiate, actualize, and refine the adaptations to colonize new fitness peaks [43].

This idea that adaptive alleles from one lineage can set the stage for further diversification of more lineages also underlies some general hypotheses about adaptive radiations, such as the hybrid swarm and syngameon hypotheses – in which radiations are driven by the exchange of genetic variation either from distinct lineages outside the radiation or within the radiation itself [44–46]. There is a wealth of evidence for extensive histories of hybridization in radiations (e.g. [47–53]), that suggests radiations are fueled by diversity that was generated across many lineages. Well documented cases of exchanges of adaptive variation aiding further diversification within a radiation include the exchange of beak shape alleles across Darwin's finches [54] and wing pattern alleles across *Heliconius* species [49,55–57] that allow multiple species to converge on similar Mullerian mimicry patterns. However, we are only just beginning

114 to explore how the introduction of genetic diversity from such groups gives recipient lineages
115 access to new fitness peaks and generates the wealth of ecological, morphological, and species
116 diversity of adaptive radiations [1,58,59]. This is necessary to fully understand the extent to
117 which diversity can self-perpetuate during the process of radiation [60].

118 An adaptive radiation of trophic specialist pupfishes on San Salvador Island in the
119 Bahamas is an excellent system for understanding how the rapid evolution of major ecological
120 transitions occur in nature. This radiation contains a wide-spread generalist pupfish species
121 (*Cyprinodon variegatus*) that occurs in sympatry with two previously described trophic
122 specialists that are endemic to many of the hypersaline lakes on the island: a molluscivore (*C.*
123 *bronotheroides*) with a novel nasal protrusion which is an oral-sheller of gastropods (St. John et
124 al. 2020) and a scale-eating specialist (*C. desquamator*) with two-fold larger oral jaws [61]. The
125 evolutionary novelties in this system originated recently; the hypersaline lakes on San Salvador
126 Island were dry during the last glacial maximum 6-20 kya years ago [62–64]. Intriguingly, we
127 recently discovered a fourth species of pupfish living in sympatry with the two specialists and
128 generalist on San Salvador Island. This species exhibits intermediate jaw morphology between
129 *C. desquamator* and *C. variegatus* (Fig 1). Furthermore, in a previous whole genome
130 resequencing study, individuals with this intermediate jaw morphology unexpectedly formed a
131 monophyletic group across lake populations distinct from *C. desquamator* using the
132 unsupervised machine-learning approach Saguaro [51,65]. Here we refer to this new ecomorph
133 as the 'wide-mouth' because its mouth is wider than any other species in the radiation. The
134 multi-peak fitness landscape driving this radiation suggests that *C. desquamator* is isolated by a
135 large fitness valley from *C. variegatus* and *C. brontotheroides* [10,66] and this intermediate
136 'wide-mouth' may provide clues how this valley was traversed.

Here we first investigate the position of the 'wide-mouth' on the ecological spectrum from generalist to scale-eating specialist using a combination of morphological, behavioral, dietary, and genomic data. We then estimated the demographic history of the 'wide-mouth' and explore the timing of selection on shared and unique genetic variation involved in adaptation to scale-eating to better understand this ecological transition. Additionally, we explore the extent to which all trophic specialist pupfishes on this island share adaptive genetic variation, despite occupying divergent ecological niches. Our results show that diversification of one species in a radiation can promote further diversification by sharing adaptive genetic variation useful for specialization.

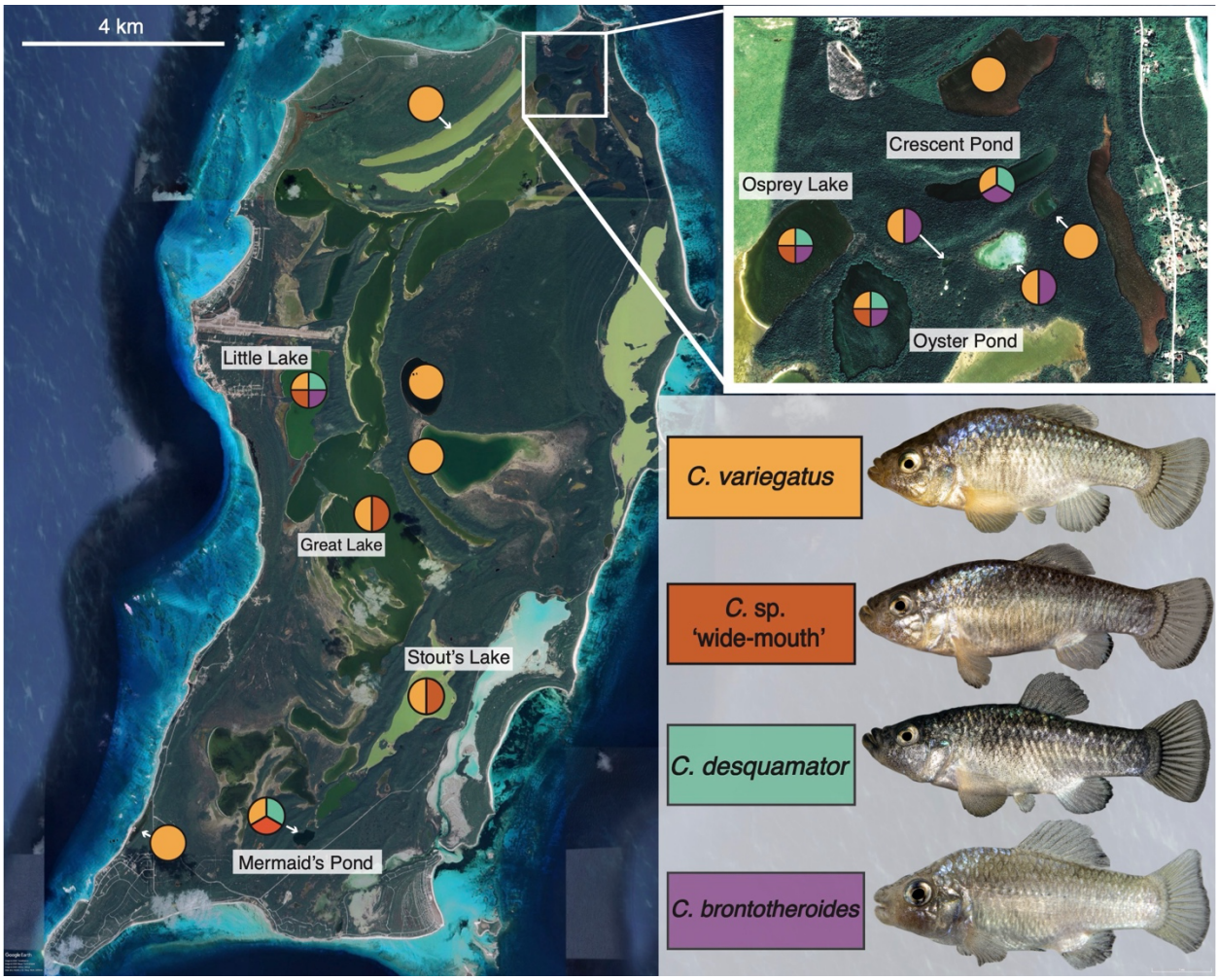

Fig. 1: Distribution of generalist, *C. brontotheriodes*, *C. desquamator*, and *C.* sp. 'wide-mouth' populations in hypersaline lakes on San Salvador Island. Pie charts indicate the presence of sympatric *Cyprinodon* species in each lake and are color-coded with representative pictures of generalist *C. variegatus* (gold), recently discovered *C.* sp. 'wide-mouth' ecomorph (red-orange) with intermediate jaws, scale-eater *C. desquamator* (teal) with the largest oral jaws, and molluscivore *C. brontotheroides* (purple) with characteristic nasal protrusion. Labeled lakes contain all known *C.* sp. 'wide-mouth' populations sampled for this study. Satellite image from Google Earth.

Results

Wide-mouth ecomorph is ecologically intermediate and morphologically distinct

We found the 'wide-mouth' ecomorph to be morphologically distinct from *C. desquamator* and *C. variegatus* across a suite of craniofacial traits (Fig. 2A-B). The lower jaw length of 'wide-mouth' was intermediate between *C. desquamator* and *C. variegatus* (Fig. 2C), while the buccal width and adductor mandibulae height were 8% larger in 'wide-mouth' than *C. desquamator* (Fig. 2E-F). These morphological differences were consistent across lakes that contained all three species (Osprey and Oyster) and within Great Lake which contained only 'wide-mouth' and generalists (Fig S1). Trait differences in the 'wide-mouth' were heritable in a common garden laboratory environment after one generation: 'wide-mouth' displayed 4% larger buccal width and 2% larger adductor mandibulae insertion height in the lab environment than *C. desquamator* (Fig S2).

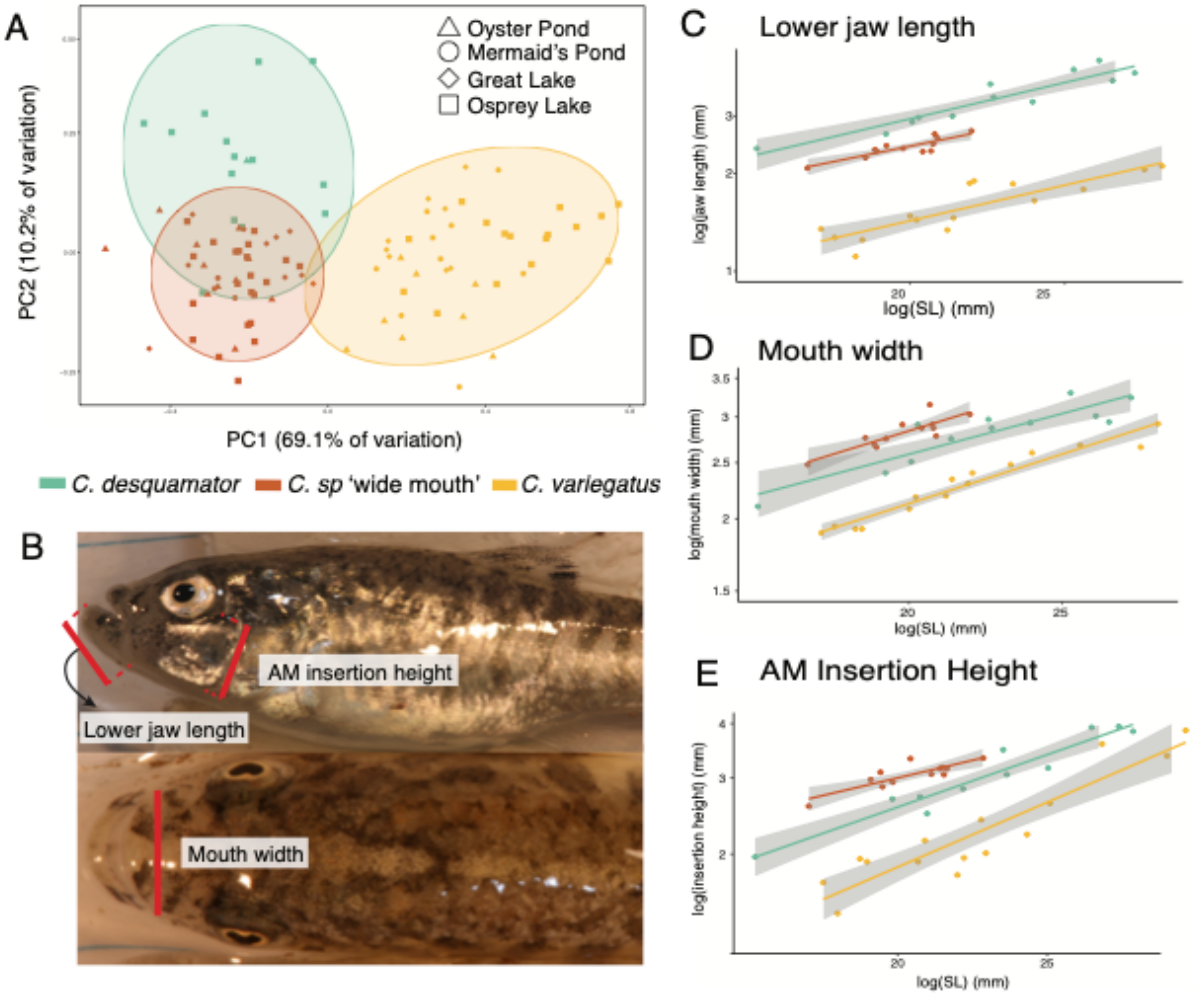

Fig 2. The *C.* sp. 'wide-mouth' ecomorph has distinct morphology within the San Salvador Island adaptive radiation across multiple traits. A) First two principal components of morphological diversity for 8 size-corrected traits and 95% confidence ellipses by species (*C. variegatus* : gold; *C.* sp. 'wide-mouth': red-orange; *C. desquamator*: teal; *C. brontotheriodes* not shown). Shapes of points represent different lakes. PC1 is mainly described by lower jaw length and PC2 by adductor mandibulae insertion height, buccal width, and neurocranium width. B) Depictions of the three external measurements that best distinguished *C.* sp. 'wide-mouth' from both *C. desquamator* and *C. variegatus*, measured using digital calipers. C-E) The relationship between standard length (mm) of individuals and their C) lower jaw length, D) buccal cavity

width, and E) adductor mandibulae insertion height (AM insertion) across individuals of the three species in Osprey Lake. 95% confidence bands for linear models in gray.

'Wide-mouth' occupies a distinct intermediate scale-eating niche

We found that 'wide-mouth' ingest scales, but at a significantly lower frequency than C. *desquamator* (Wilcoxon Rank Sum test, $P = 0.004$; Fig. 3A). We did not detect any scales in *C. variegatus* guts (Fig 3A). A previous gut content analysis of more individuals also found nearly zero occurrence of scales in the *C. variegatus* diet [67]. All three sympatric species from Osprey Lake collected on the same day from the same site differed in δ15N levels (ANOVA, $P > 1.29\text{x}10^{-7}$; Fig. 3B); 'wide-mouth' δ15N was intermediate between *C. variegatus* and *C. desquamator* (Tukey HSD; P=0.04 & 0.03 respectively). Similarly, high-speed scale-eating strikes on euthanized fish prey indicate an intermediate lower jaw angle in the 'wide-mouth' relative to generalist and scale-eating strikes (Fig. 3C; also see St. John et al. 2019 for analysis of scale-eating strikes relative to generalist).

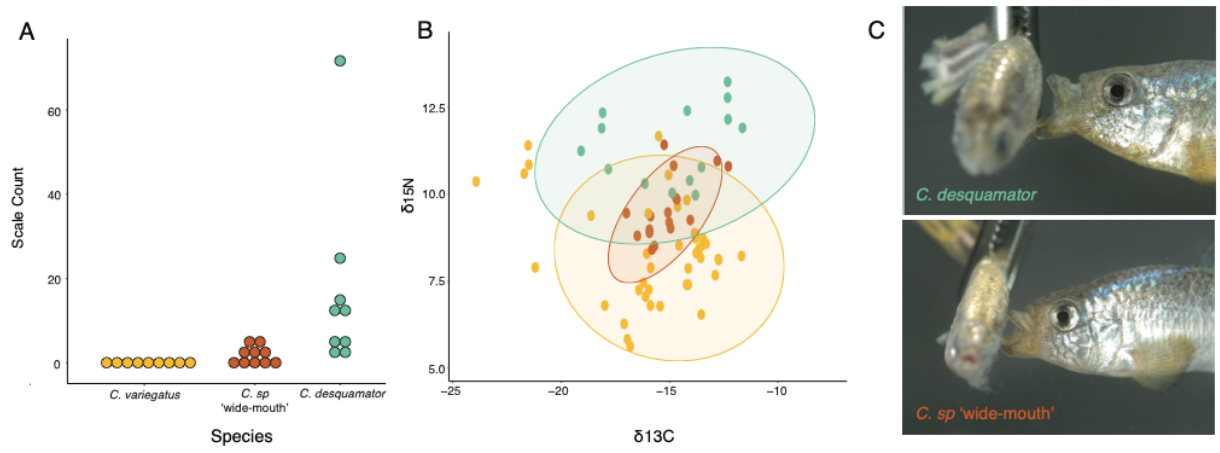

Fig. 3: The *C.* sp. 'wide-mouth' individuals ingest scales. A) Dot plot of individual scale counts from gut content analysis of the hindgut of Osprey pupfish populations (10 individuals per species). B) Individual variation in relative trophic position (δ15N stable isotope ratio) and

198 dietary carbon source (δ13C stable isotope ratio) with 95% confidence ellipses for the three
199 species. C) Still images from Phantom VEO high-speed videos (1,100 frames per second) of
200 scale-eating strikes in *C. desquamator* and *C.* sp. 'wide-mouth'. Note the distinct lower jaw
201 angle with the suspensorium at the point of impact with the prey.
202
203 ***'Wide-mouth' did not result from hybridization between* variegatus *and* desquamator**
204 We tested whether 'wide-mouth' was the product of recent hybridization. First, extensive multi-
205 year sampling efforts show that 'wide-mouth' populations are not found in every lake where both
206 *C. variegatus* and *C. desquamator* are present (e.g. Crescent Pond; Fig. 1). However, we
207 explored this possibility in more depth by resequencing 24 genomes of 'wide-mouth' across lake
208 populations and comparing these to 86 resequenced genomes of *C. variegatus*, *C.*
209 *brontotheriodes*, and *C. desquamator* from a previous study [68].
210 Several lines of genomic evidence support the 'wide-mouth' ecomorph as a distinct
211 species. First, 'wide-mouth' individuals do not occupy an intermediate position between *C.*
212 *desquamator* and *C. variegatus* along either of the first two principal components that represent
213 the major axes of genetic variation in the radiation. Instead, 'wide-mouth' occupy a distinct
214 cluster relative to the other three species (Fig. 4A). This is further corroborated by the model-
215 based approach of ADMIXTURE, in which 'wide-mouth' individuals share more ancestry with
216 each other than with either *C. desquamator* or *C. variegatus* under the two most likely K values
217 based on cross-validation error estimates (K=6 and 7; Fig. 4B). This pattern holds when we
218 decrease or increase the K value used in the analysis to model more or less population structure
219 within groups (Fig. S3). Lastly, we used formal tests for introgression and admixed populations,
220 f_3 and f_4-statistics, to assess the evidence that 'wide-mouth' are the byproduct of recent

221 admixture. The significant positive f_3-statistics and the non-significant f_4-statistics support our
222 inference that the 'wide-mouth' is not a recent admixed population of any pairwise combinations
223 of the *C. brontotheriodes*, *C. variegatus*, or *C. desquamator* populations (Table S1).
224
225 ***'Wide-mouth' and* C. desquamator *populations are sister species which diverged shortly after***
226 ***the onset of adaptive radiation on San Salvador Island***
227 To better understand the history of divergence and gene flow among the four species on San
228 Salvador Island, we used *fastsimcoal2* [69] to run coalescent simulations and compare 28
229 different demographic models of divergence and gene flow on San Salvador Island (Table S2).
230 These models represented all possible topologies among the four species and explored zero,
231 early, and current gene flow scenarios. We evaluated their fit against our empirical site frequency
232 spectrum (SFS) calculated from populations of the four species that occur in sympatry in Osprey
233 Pond.
234 In the best supported model, 'wide-mouth' was sister to *desquamator* with current gene
235 flow and a divergence time estimate of 11,658 years ago (95 CI: 8,257-20,113 years; Fig 4C-D)
236 (Table 1 and S2). This model indicates that the ancestor to 'wide-mouth' and *C. desquamator*
237 populations first diverged from *C. variegatus* 15,390 years ago (95% CI: 10,722-23,927
238 years;Fig 4D). This estimate of the origin of the radiation overlaps well with geological age
239 estimates based on the filling of hypersaline lakes on San Salvador Island after the end of the last
240 glacial maximum period (~6-19K years ago; [62–64]). *C. variegatus* and *C. brontotheriodes*
241 populations in Osprey Lake diverged much more recently than the two scale-eating populations
242 462 years ago (95% CI: 411-1,121 years; Fig 4D).
243

244 Table 1. Support for the five best-fitting demographic models for the evolution of the *C.* sp.
245 'wide-mouth' from the site frequency spectrum. The likelihood and AIC scores for the top five
246 best-fitting models estimated in *fastsimcoal2* for the Osprey populations of *C. variegatus* (var),
247 *C. brontotheroides* (bro), *C. desquamator* (des), and *C.* sp. 'wide-mouth' (wid) are presented
248 here with a complete list of all models tested reported in Table S2. Change in likelihood (ΔLnL)
249 represents the difference in likelihood from the expected simulated SFS in the demographic
250 model tested. Change in AIC (ΔAIC) represents the difference in AIC scores from the model
251 with the smallest ΔAIC. All models presented here represent different divergence scenarios with
252 recent gene flow allowed, which were better supported than models with no gene flow or early
253 gene flow. Visual representations of the top five models are depicted in Figure S5.

254

Divergence Model	LnL	ΔLnL	AIC	ΔAIC
(1) ((des,wid),(bro,var)) + (des,wid) diverges first + recent gene flow	-11701	1077	54133	0
(2) ((des,bro),var),wid)) + recent gene flow	-11780	1112	54296	35
(3) ((des,bro),wid),var)) + recent gene flow	-11806	1138	54418	61
(4) ((bro,wid),des),var)) + recent gene flow	-11808	1140	54423	63
(5) ((des,wid),(bro,var)) + (bro,var) diverges first + recent gene flow	-11846	1178	54602	101

255

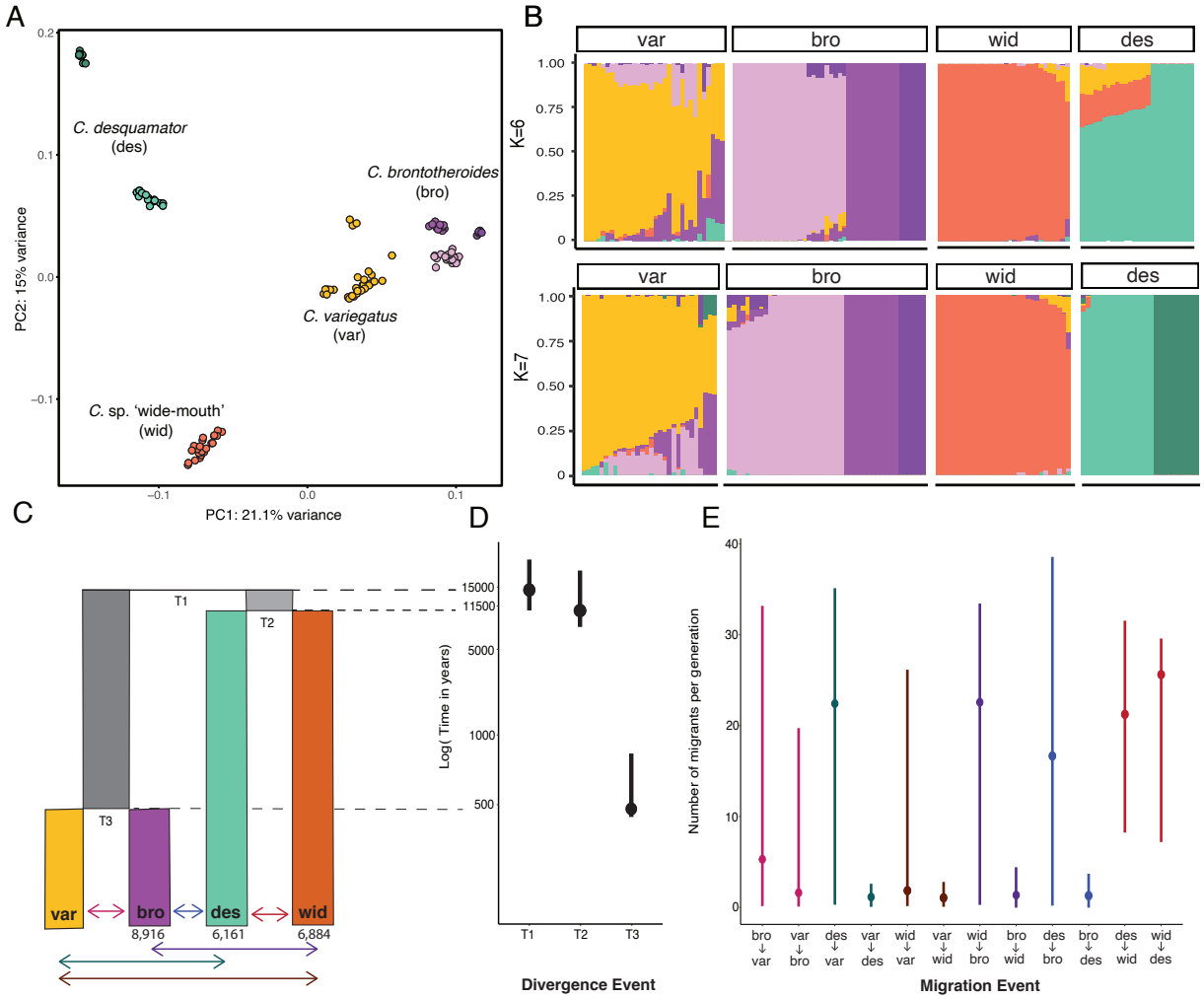

Fig 4. *C.* sp. 'wide-mouth' population did not result from recent hybridization. A) Principal components analysis of the four focal groups on San Salvador Island based on an LD-pruned subset of genetic variants (78,840 SNPs). B) Ancestry proportions across individuals of the four focal groups. Proportions were inferred from ADMIXTURE analyses with 2 values of K with the highest likelihood on the same LD-pruned dataset in A. C) Best supported demographic model in which *C. desquamator* diverged from the *C.* sp. 'wide-mouth' based on an LD-pruned dataset with no missing information across all Osprey Lake individuals (67,400 SNPs). Divergence time is shown with the maximum likelihood point estimate from the run with the best fit and the 95% confidence interval for that parameter estimate based on 100 bootstrap replicates. D) Maximum

266 likelihood point estimate and 95% confidence intervals for migration rate parameters involved in
267 the best fitting model depicted in units of the number of migrants per generation.
268
269
270 ***Shared signatures of selection across the three specialists in the radiation***
271 Next, we investigated whether the evolution of new trophic specialists on San Salvador Island
272 may have been aided by reuse of the same underlying genetic variation. We characterized
273 regions of the genome under selection in the Osprey Lake populations of the four species using
274 the sliding window SFS-based approach SweeD (Pavlidis et al. 2013) and neutral simulation
275 thresholds based on demographic changes in effective population size over time (Fig S4; Table
276 S3). A higher percentage of the genome was under positive selection in all specialist populations
277 compared to the *C. variegatus* population (Fig 5A). This pattern might be expected given the
278 divergent selection pressures the specialists face to adapt to different trophic niches. Of all the
279 specialists, *C. brontotheriodes* exhibited both the most selective sweeps and the longest selective
280 sweeps (Fig 5A). This suggests that *C. brontotheriodes* have undergone selection most recently
281 among all the species in Osprey Lake and is supported by the recent divergence time between the
282 *C. brontotheriodes* and *C. variegatus* populations (Fig 4D).
283 Additionally, we assessed patterns of genetic divergence across the four species in
284 Osprey Lake. Allowing for some level of gene flow between species, we calculated the number
285 of fixed and nearly-fixed SNPs (Fst $\geq$ 0.95) between all pairwise combinations of populations in
286 Osprey Lake. All specialists, including the two scale-eating species, were more genetically
287 diverged from each other than to *C. variegatus* species based on the number of SNPs fixed or
288 nearly-fixed between them (Fig 5B). This pattern of stronger genetic divergence between

specialists also held across fixed SNPs, the top 1% of F_{st}, and genome-wide average F_{st} (Table S4). Next, we identified a set of candidate adaptive alleles for each specialist by filtering for SNPs that were fixed or nearly fixed (Fst ≥ 0.95) relative to *C. variegatus* and found within a hard selective sweep in the focal specialist. In this set of candidate adaptive alleles, *C. brontotheriodes* had the fewest adaptive alleles while *C. desquamator* had the most (Fig 5B).

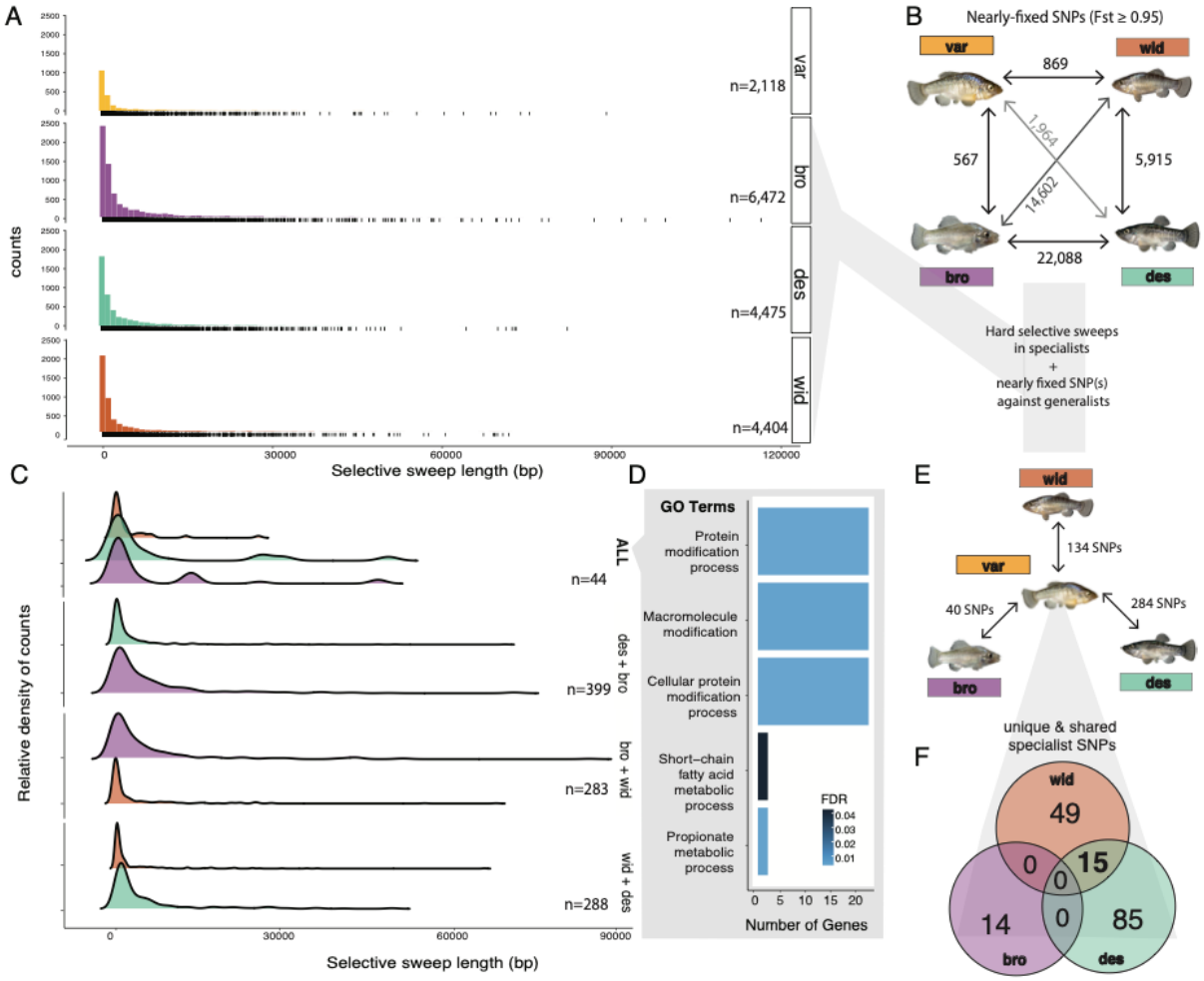

Figure 5. Patterns of selection and genetic divergence in specialist genomes. A) Histogram of selective sweep length distributions across all four San Salvador Island species. Rug plot below each histogram representing the counts of selective sweeps binned into different lengths is included to highlight the presence of several larger selective sweeps in the tails of the

distribution. B) The total number of fixed or nearly-fixed SNPs ($F_{st} \geq 0.95$) between each group in Osprey Pond. C) Ridgeline plots for length distributions of selective sweeps shared between different combinations of specialists (*C. brontotheriodes*: purple, *C. desquamator*: teal, *C.* sp. 'wide-mouth': red-orange). Full results of the GO enrichment analysis of the 57 genes contained in the shared selective sweep regions across all specialists. D) The number of adaptive alleles (nearly-fixed SNPS [$F_{st} \geq 0.95$] relative to *C. variegatus* and under selection [CLR thresholds in Table S3]) in each population of specialists in Osprey Lake. Venn diagram highlights those adaptive alleles that are unique to each specialist and shared with other specialists.

Next, we looked for shared patterns of genetic divergence and selection across the specialist genomes. Despite divergent trophic specializations and morphology, we found evidence of 44 shared selective sweeps across all three specialist populations that were not shared with *C. variegatus* populations (Fig 5C). These shared regions under selection in all specialists were significantly enriched for genes annotated for metabolic processes (Fig 5C), suggesting shared selection for a metabolism associated with a more protein-rich diet across trophic specialists (also see [70]). We also found evidence of shared selection across all pairwise combinations of two specialists. The shared selective sweeps were shorter than any of the selective sweeps unique to each of the specialists, suggesting that selection for these shared regions was not the most recent or strongest in any of the specialists (Fig 5C). We also found no shared fixed or nearly fixed ($Fst \geq 0.95$) adaptive alleles across all three specialists, although shared alleles did occur at lower frequencies ($Fst < 0.62$; Fig S6).

323

324 ***Shared and unique adaptive alleles in 'wide-mouth' and* C. desquamator**

325 We discovered that the two scale-eating populations shared a set of the same adaptive alleles not
326 found in *C. brontotheriodes* or *C. variegatus* (Fig 5D). This consisted of 15 alleles in 6 shared
327 hard selective sweeps in *C. desquamator* and 'wide-mouth': 10 SNPs were in unannotated
328 regions, two were in the introns of the gene *daam2,* and three were in regulatory regions of the
329 genes *usp50, atp8a1,* and *znf214* (one variant each).

330 Shared adaptive alleles in the gene *daam2,* a wnt signaling regulator, are intriguing
331 because knockdown of this gene causes abnormal snout morphology, osteoporosis, and changes
332 in insulin and alkaline phosphate levels in mice [71], and abnormal cranial and skeletal
333 development in zebrafish (Kida et al. 2007). Craniofacial morphology is one of the rapidly
334 diversifying traits in this system, suggesting that divergence in *daam2* may play a role in the
335 shared craniofacial divergence of the two scale-eating species. Similarly, *usp50* functions in
336 protein metabolism and deubiquination [72] and may play a role in shared metabolic adaptations
337 to the higher-protein content of a scale-eating or snail-eating diet (also note microbiome
338 divergence of *C. desquamator* with increased prevalence of collagenase-digesting bacteria when
339 reared in a common garden:[73]). *atp8a1* is an ion transporter [74], *znf214* is a transcription
340 binding factor, and the ten unannotated variants were not associated with lower jaw size
341 variation in a previous genome-wide association study of the radiation (Richards et al. 2021).

342 Despite the divergent craniofacial features of the 'wide-mouth', none of the adaptive
343 alleles unique to the 'wide-mouth' appear to be in or near genes annotated for craniofacial
344 phenotypes in model organisms. In *C. desquamator,* three of the 13 sets of unique adaptive
345 alleles are in or near genes annotated for craniofacial phenotypes: a *de novo* non-synonymous

346 coding substitution in the gene *twist1*, several putative regulatory variants near the gene *gnaq,*
347 and 8 variants in and near the gene *bri3bp*, which is located inside a QTL region for cranial
348 height in pupfish (St. John et al. 2021). In *C. brontotheriodes*, there is also a candidate
349 craniofacial adaptive allele: a non-synonymous coding substitution in the gene *kat6b*, which is
350 associated with abnormal craniofacial morphologies, including shorter mandibles in mice [75,76]
351 and Ohdo Syndrome and bulbous noses in humans [77].
352 This pattern of unique alleles relevant to craniofacial phenotypes in *C. brontotheriodes*
353 and *C. desquamator*, but not 'wide-mouth', holds if we lower the threshold to the top 1
354 percentile of F_{st} between specialists and generalist. 'Roof of mouth development', 'bone
355 development' and 'skeletal system development' are in the top 20 most significantly enriched
356 GO terms for *desquamator* candidate adaptive alleles, with 6 significantly enriched terms
357 relevant to cranial and skeletal development (out of 165 enriched terms total). Similarly,
358 'embryonic skeletal system development' and 'skeletal system development' were significantly
359 enriched terms for *brontotheriodes* candidate adaptive SNP alleles (out of 8 enriched terms
360 total). However, 'wide-mouth' adaptive alleles at this lower F_{st} threshold were not significantly
361 enriched for any GO terms related to craniofacial or skeletal morphology (n=52 terms; Fig S7).
362
363 *Selection for adaptive alleles shared in both scale-eating populations preceded selection for*
364 *adaptive alleles unique to C. desquamator*
365 Additionally, we estimated the timing of selection on unique and shared adaptive alleles in
366 'wide-mouth' and *desquamator* to explore the evolution of scale-eating in this system. Previous
367 studies indicate that the *C. desquamator* scale-eater phenotype is separated from *C. variegatus*
368 generalist niche by a deep fitness valley on the adaptive landscape (Martin and Gould 2020;

369 Martin and Wainwright 2013), suggesting a difficult ecological transition. Adaptation to an
370 intermediate scale-eating niche such by the 'wide-mouth' lineage may have provided an easier
371 first step and the adaptive alleles involved may have set the stage for the more specialized scale-
372 eater *C. desquamator* to evolve. To test this, we estimated the age at which the adaptive alleles
373 first started sweeping in each population using the coalescent-based approach starTMRCA [78].
374 Across the 30 sets of adaptive alleles with selective sweep ages, we found an overall
375 difference in timing of selection between shared and unique adaptive alleles in the two scale-
376 eater populations (ANOVA *P*-value = 0.00478). In *desquamator*, shared adaptive alleles were
377 under selection before any unique adaptive alleles (Tukey HSD *P*-value = 0.003217; Fig. 6). We
378 found a similar trend in 'wide-mouth': shared adaptive alleles were generally under selection
379 before those unique to the species (Fig. 6). However, this difference was not significant due to
380 one set of unique adaptive alleles near the gene *slitrk5* which was the oldest estimated sweep
381 (ANOVA, Tukey HSD; *P* = 0.8367).
382 In contrast to our predictions, selection on 4 of the 6 shared sets of adaptive alleles
383 occurred significantly earlier in *desquamator* than 'wide-mouth'. Only a single set of these
384 adaptive alleles had an older median age estimate in 'wide-mouth' than *desquamator*, although
385 the 95% HPD intervals surrounding these point estimates overlapped between the two
386 populations (Fig. 6). The other adaptive allele set that had overlapping 95% HPD intervals
387 between the two populations were a set of unannotated de novo mutations.
388

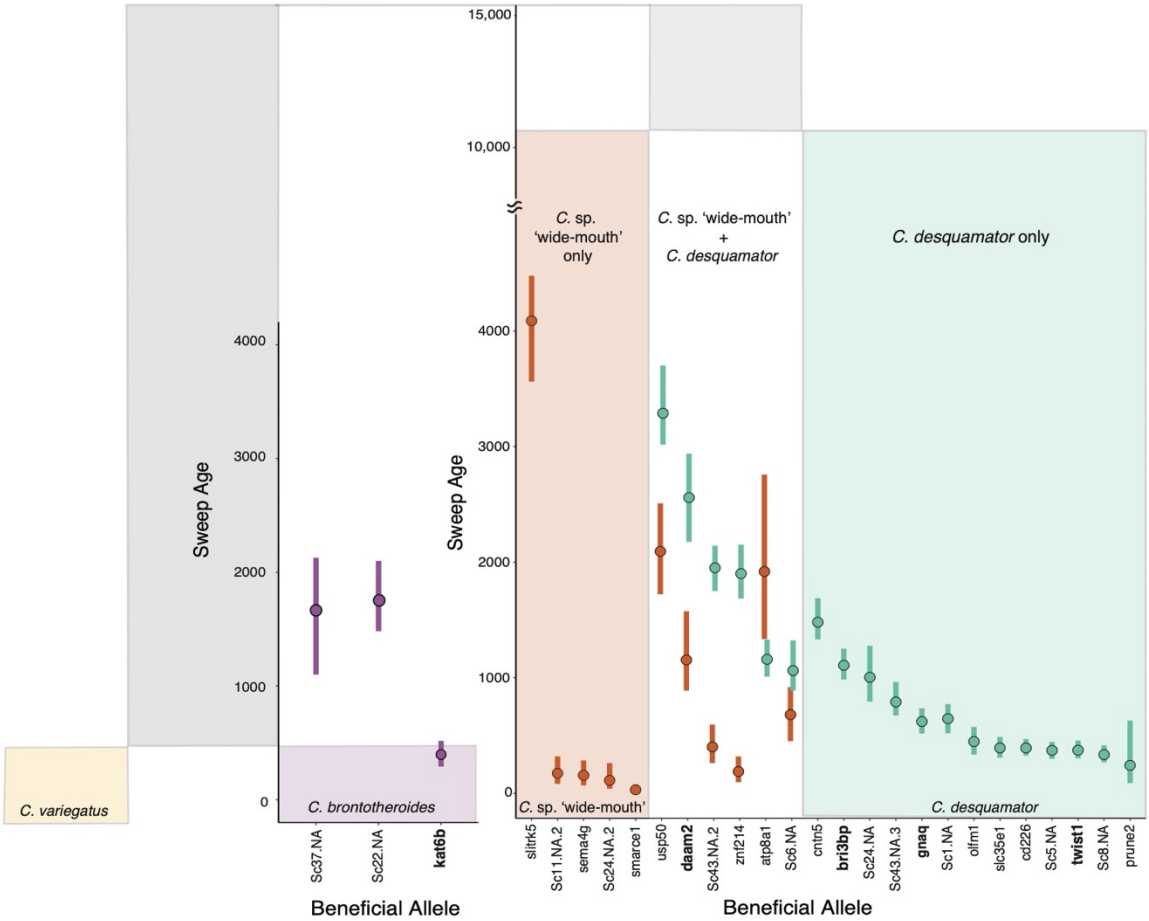

Fig 6. Timing of selection on adaptive alleles in trophic specialists nested within the species demographic history. The mean and 95% HPD estimates for the timing of selection on sets of fixed or nearly fixed SNPs (named by the gene they are in or within 20-kb of) for *C. desquamator*, *C.* sp. 'wide-mouth', and *C. brontotheroides* populations found in sympatry in Osprey Lake (sweeps in *C. variegatus* not shown). The age of each beneficial allele is color coded by the species it swept in and the inferred demographic history is displayed in the background for comparison. Gene names highlighted in bold are associated with oral jaw size in model organisms.

399 *Shared adaptive variation may have resulted from introgression between desquamator and*
400 *'wide-mouth' scale-eaters*
401 Finally, we explored several selection scenarios surrounding the shared adaptive alleles between
402 'wide-mouth' and *desquamator*. The most parsimonious answer for why these two populations
403 share adaptive alleles is that these alleles swept in their common ancestor and were retained in
404 both post divergence. However, the timing of selection on these alleles is much more recent in
405 both populations than the inferred divergence time (Fig 6), suggesting that these alleles were not
406 selected upon in their most recent common ancestor. Second, the timing of selection on most of
407 these shared adaptive alleles is significantly different between the populations (Fig 6), suggesting
408 that these alleles were not selected upon in a single event in the shared ancestor. This left us to
409 explore two other scenarios that could explain the shared adaptive alleles: 1) these alleles were
410 segregating in both populations after they initially diverged from each other and independently
411 swept to fixation or 2) these adaptive alleles introgressed from one population to another after
412 being selected for in one population.
413 To distinguish between these two scenarios, we assessed the regions surrounding these
414 shared adaptive alleles for signatures of introgression. Introgression between recently diverged
415 sister species is often more challenging to detect in comparison to introgression with a more
416 distantly related outgroup because of the high genetic similarity between sister species.
417 However, introgression between sister species can be detected from population level
418 polymorphism data by looking for regions of the genome with lower absolute genetic divergence
419 than expected given the genome-wide average [79–82]. We thus calculated D_{xy} in sliding
420 windows across the genomes of the Osprey Lake populations and compared the distribution of
421 D_{xy} values in the regions surrounding the shared adaptive alleles to the distribution of D_{xy} values

422 across the genome. The average D_{xy} of the shared adaptive alleles was two times lower than
423 average genome-wide values between *desquamator* and 'wide-mouth' (Fig 7A). It was also
424 slightly lower (1.2X) than the average D_{xy} for all selective sweep regions in the 'wide-mouth'
425 genomes, suggesting it is not due to selection on these regions in general (Table S5). This lower
426 D_{xy} was predominantly due to four out of the six regions containing shared adaptive alleles
427 having ~2-5 times lower D_{xy} values than the genome-wide average. The other two regions had
428 comparable (*znf214*) and higher (unannotated region on scaffold 43) D_{xy} values than the genome-
429 wide average (Fig 7B). The lower genetic distance between *C. desquamator* and the 'wide-
430 mouth' in these adaptive regions suggests they may have introgressed between the two groups
431 rather than independent selection on ancestral polymorphisms since they diverged approximately
432 11,000 years ago.
433
434

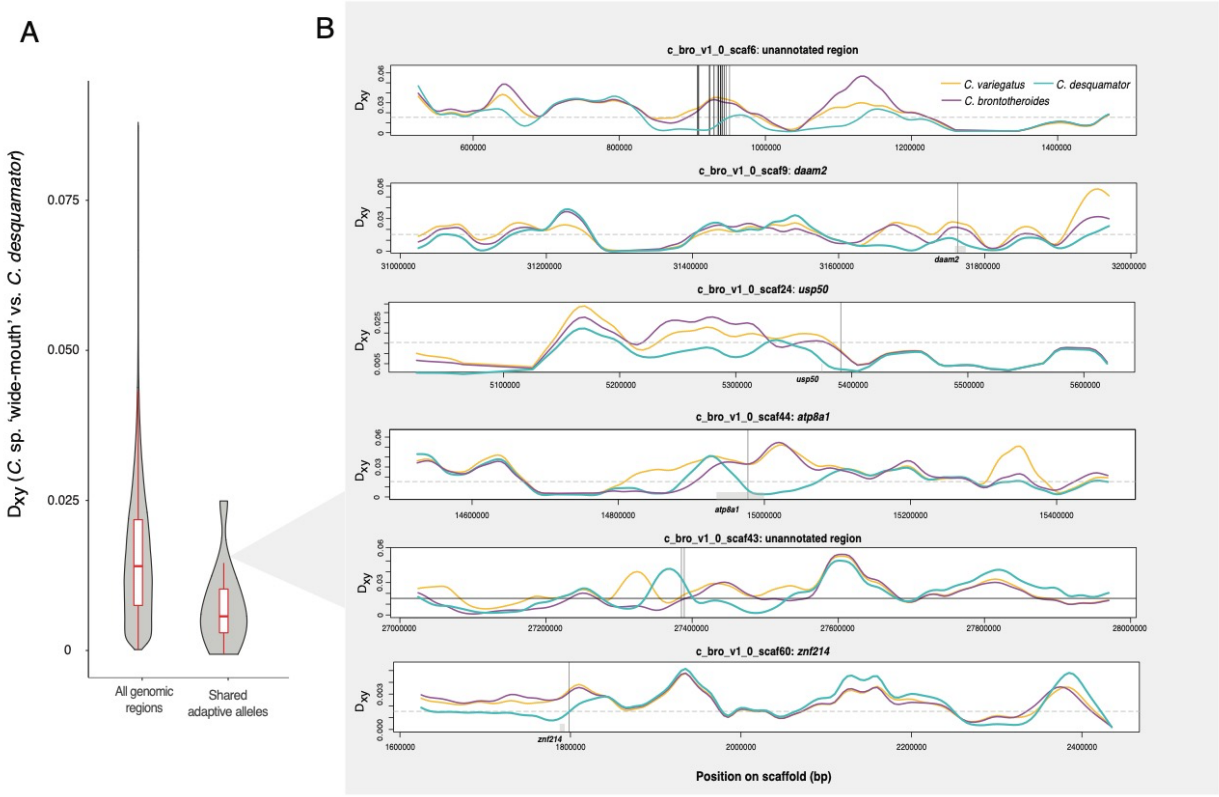

Fig. 7. Absolute genetic divergence between 'wide-mouth' and *desquamator*. A) Distribution of D_{xy} values across 20-kb regions for the whole genome and regions with adaptive alleles shared between *desquamator* and 'wide-mouth'. B) D_{xy} values across the 1 million base pairs surrounding the six regions of shared genetic variation between *desquamator* and 'wide-mouth'. Vertical solid black lines indicate the position of the shared adaptive alleles between 'wide-mouth' and *desquamator*, horizontal dashed gray lines represent the genome-wide average D_{xy} between *desquamator* and 'wide-mouth'. The smoothed lines represent D_{xy} between *C. desquamator* and *C.* sp. 'wide-mouth' (teal), *C. brontotheriodes* (purple), and *C. variegatus* (gold) across these portions of the scaffold. The D_{xy} values were summarized with smoothed splines using the smooth.spline() function in R for ease of visualization across the different comparisons. Gray boxes represent the nearest gene to the adaptive alleles and unannotated

447 adaptive alleles were those in which no gene was located within 20-kb of the SNP (an
448 approximate LD estimate from a previous study; [68]).
449
450
451 **Discussion**
452 *Discovery of a new cryptic scale-eater evolved through reuse of shared adaptive alleles*
453 The hallmark of adaptive radiation is a rapid burst of diversification which is predicted by theory
454 to slow down over time as niche width driving further divergent selection diminishes (Martin and
455 Richards 2019). An alternative possibility is that radiations can be self-propagating and that the
456 diversity generated within the first stages of radiation helps beget further diversity [60]. This
457 could happen through exploitation of new trophic levels created by new species (Seehausen et al.
458 2019) or physical alterations of the environment by new species (niche construction) that may
459 create additional opportunities for speciation (reviewed in [1,58]). The diversity begets diversity
460 hypothesis can be visualized as the exploration of a complex multi-peaked fitness landscape; as
461 species in the radiation colonize new peaks, this provides access to additional neighboring fitness
462 peaks to fuel rapid radiation.
463 At the microevolutionary level, shared adaptive variants can also help other populations
464 colonize new or ecologically similar areas of the fitness landscape. However, the genetic basis
465 and microevolutionary processes underlying major ecological transitions are still poorly
466 understood in nature. Our discovery of a cryptic new scale-eating species through morphological,
467 dietary, and genomic analyses revealed shared selective sweeps among all three trophic
468 specialists in a radiation of pupfishes despite the divergent morphological and ecological
469 adaptations between them. However, only in the two scale-eating populations, *C. desquamator*

470 and *C.* sp. 'wide-mouth', did we find shared nearly-fixed or fixed adaptive alleles. These species
471 are sister species, suggesting a single origin for scale-eating. Nonetheless, these shared adaptive
472 alleles were not selected upon in the ancestral population and swept first in the *C. desquamator*
473 population. This contradicts our initial prediction that the evolution of the intermediate 'wide-
474 mouth' scale-eater would aid the evolution of the more specialized scale-eater *C. desquamator*.
475 Instead, adaptive alleles from *C. desquamator* may have introgressed and then selected upon in
476 the 'wide-mouth' population. Additionally, unlike *C. brontotheriodes* and *C. desquamator*, the
477 cryptic 'wide-mouth' appears to have little unique genetic variation relevant to craniofacial
478 morphology, which is a major axis of diversification in the other trophic specialists [83]. An
479 intriguing implication of these findings is that adaptive variants within one specialist may aid the
480 evolution of another into a similar niche and promote further ecological divergence within
481 radiations, in line with the diversity begets diversity hypothesis [60].
482
483 *An adaptive walk underlies the major ecological transition from generalist to scale-eating*
484 *specialist*
485 One of the foundational models of adaptation is that it proceeds in 'adaptive walks' towards
486 fitness optima that involve the sequential fixation of adaptive alleles that move a population in
487 the phenotypic direction of the local optimum [84–88]. The distinct timing of selection across
488 different adaptive alleles suggests that the ecological transition from generalist to novel scale-
489 eating specialist involved such an adaptive walk rather than a sudden burst of concurrent
490 selection events after some major environmental shift. These distinct, multiple bouts of selection
491 could be caused by mutation-limited (i.e. waiting for new beneficial alleles; [89–91]) or
492 mutation-order processes (i.e. epistatic interactions; [92–94].

We found that all of the shared adaptive alleles between the scale-eating populations occurred at low frequency in generalist populations on other Caribbean islands in a previous study ([68]; Table S7). For example, three copies of the shared *usp50* adaptive allele were found outside of San Salvador Island (Table S7). This indicates that initial bouts of selection occurred on available standing genetic variation and that staggered timing of hard selective sweeps in each trophic specialist most likely reflects mutation-order processes in which selection on a beneficial allele was contingent on prior fixation of other adaptive alleles in each specialists' genetic background. However, several adaptive alleles originated from introgression or de novo mutations found only on San Salvador Island (Table S7), so part of the adaptive walk may have also been mutation-limited.

Cryptic scale-eating species reveals features of the adaptive walk towards scale-eating specialization

Although the two scale-eating species shared a set of adaptive alleles and a recent common ancestor, 5 of 6 shared adaptive regions swept at significantly different times between the two species. This difference in timing may result from several different scenarios: 1) independent adaptive walks to the same scale-eating niche, 2) independent adaptive walks to different scale-eating niches or 3) the adaptive walk of one population depends on the adaptive walk of the other population. We explore each of these scenarios in turn.

First, the difference in timing of selection on the same shared adaptive alleles could indicate independent adaptive walks to the same scale-eating peak that occurred at different times and/or by slightly different routes. *C. desquamator* and 'wide-mouth' populations have

516 predominantly abutting ranges, with only a small amount of geographic overlap on San Salvador
517 Island in four lakes, Osprey, Oyster, Little Lake, and Mermaid's Pond (Fig 1). If this current
518 distribution is representative of their historical ranges and the two lineages began diverging
519 about 11,000 years ago, it is possible that the adaptive walks took place in different lakes and
520 were largely independent of one another. The differences in timing on the shared adaptive alleles
521 and the presence of unique alleles observed in each population are reminiscent of mutation-order
522 speciation [93,95]. In mutation-order speciation the same alleles are favored in populations that
523 are adapting to similar environments, yet by chance and/or epistatic interactions with different
524 genetic backgrounds, similar adaptive alleles fix in just one population. At least one set of alleles
525 near the gene *slitrk5* are unique to the 'wide-mouth' scale-eater and fixed well before selection
526 occurred on the shared adaptive variants between the two scale-eater populations (Fig 5).
527 Epistatic interactions of these *slitrk5* alleles may have prevented the 'wide-mouth' from fixing
528 additional segregating alleles that are uniquely fixed in *C. desquamator.*
529 Second, the difference in timing of selection may have occurred because the two scale-
530 eating populations are adapting to two different scale-eating niches. The intermediate diet,
531 distinctly sized morphological traits, and smaller body size in the 'wide-mouth' scale-eater
532 compared to *C. desquamator* may indicate the 'wide-mouth' scale-eater is adapting to a different
533 scale-eating niche. While the two scale-eating populations do share some overlap in adaptive
534 alleles and selective sweeps, the majority of selective sweeps are unique to each species (Fig 5 &
535 6), including neurogenesis, brain, and nervous system development (*slitrk5, sema4g, and*
536 *smarce1*), whereas unique adaptive alleles in *desquamator* include craniofacial development
537 annotations (*olfm1, gnaq, twist1*) as well. This difference in gene annotations can also be seen at
538 the broader level of regions of the genome under selection (Fig S7). Therefore, the differences in

539 timing at shared adaptive alleles might reflect differences in relative strength of selection due to
540 different selective regimes experienced by the two scale-eating populations. While starTMRCA
541 is fairly robust in its timing estimates to different strengths of the selection [78], we cannot rule
542 out that differences in relative timing of selection might partially reflect differences in strength of
543 selection occurring in the two scale-eating populations.

544 Third, another scenario that could have led to the older timing of selection across shared
545 adaptive alleles in *desquamator* than 'wide mouth' is one in which the adaptive walk of one
546 population depended on adaptive alleles from another. The significantly older timing of
547 selection in *desquamator* on shared adaptive alleles and the low absolute genetic divergence
548 between these two scale-eating population in these regions (Fig 6) suggests that these alleles may
549 have introgressed between the two populations. Given that these shared adaptive alleles appear
550 as standing genetic variation across Caribbean populations, albeit at very low frequency in our
551 sampling, it is likely that the shared alleles were present in the ancestor and were segregating in
552 both populations after they diverged. There are several reasons why adaptive introgression may
553 have been necessary for adaptive divergence of 'wide-mouth' despite the alleles initially
554 segregating in the ancestral population. In line with mutation-order processes (e.g. Mani and
555 Clarke 1990; Schluter 2009; Good et al. 2017), these alleles might not have been adaptive until
556 the right genetic background was present in the 'wide-mouth'. Introgression from *C.*
557 *desquamator* in which the allele was already swept to high frequency could have raised the
558 frequency of these alleles in 'wide-mouth' and increased the likelihood of fixation for the
559 beneficial alleles (reviewed in [96]). This is consistent with previously proposed hypotheses for
560 how diversity begets further diversity in adaptive radiations (Whittaker 1977; Stroud and Losos
561 2016; Martin and Richards 2019).

562

563 *Shared aspects of genomic landscape of selection among all specialists additionally supports*
564 *specialization promoting further specialization*

565 Intriguingly we also find evidence of selective sweeps shared across all three specialists despite
566 their divergent adaptations and lack of a shared specialist ancestor. However, there are no
567 commonly shared adaptive alleles fixed against *C. variegatus* in these shared selective sweep
568 regions. Hard selective sweeps indicate a selection scenario in which a single beneficial allele of
569 large effect on a trait is swept to high frequency (reviewed in [97]). The lack of highly divergent
570 alleles in these regions might indicate polygenic selection events underlie the shared signatures
571 across specialists. The broad-scale transition from dietary generalist to dietary specialist may
572 involve polygenic selection with small shifts in the frequency of many alleles. Despite very
573 different expectations about the genetic basis of adaptation, polygenic selection events may have
574 been detected as a hard selective sweep in this study as the two selection types can be
575 challenging to distinguish based solely on patterns of genetic variation [98–101]. Recently
576 developed frameworks provide additional criteria to help distinguish between the two selective
577 regimes [99] but are beyond the scope of this current study.

578 These shared selective sweeps across all specialists are not the longest selective sweeps
579 in any of the specialist genomes (> 50-kb; Fig 5C), indicating they are not the most recent or
580 strongest selection events. However, these shared selective sweeps appear to be relevant to
581 dietary specialization as these regions are enriched for genes annotated for metabolic processes
582 such as short chain fatty acid and propionate metabolism (Fig 5). Propionates and other short
583 chain fatty acids are common microbiome metabolites [102]. A recent microbiome study in lab-
584 reared populations found that *C. desquamator* microbiomes appear enriched for

585 *Burkholderiaceae* bacteria that can digest collagen, further supporting an adaptive role for
586 microbiomes in the radiation [73].
587 We also see pairwise shared selective sweeps between all combinations of two
588 specialists. In contrast to the sweeps shared between all specialists, we see stronger genetic
589 divergence among species in these regions and a proportion of the selective sweeps shared
590 between two specialists do contain fixed or nearly-fixed alleles. However, the specialists that
591 share selective sweeps in these regions are fixed for different adaptive alleles, consistent with
592 previously observed patterns of parallel differential gene expression in specialists despite
593 divergent genotypes [70]. These alleles were possibly under balancing selection in the ancestor
594 (most of these alleles are segregating at intermediate frequency in *C. variegatus* currently) and
595 the alternate alleles were driven to fixation between the specialists during their respective
596 divergences. While the species have discrete phenotypes across several morphological traits
597 important to divergence in this system, these traits often lie on a continuous axis (i.e. shorter oral
598 jaw lengths in *C. brontotheriodes*, intermediate jaw lengths in *C. variegatus*, and longer oral jaw
599 lengths in 'wide-mouth' and *C. desquamator*). Some of the alleles that are alternatively fixed
600 between specialists at the same position may have incomplete dominance effects on such traits.
601 In line with adaptation to divergent trophic niches across the species, we do still see many
602 unique signatures of selection among the specialists. The *C. variegatus* population had the fewest
603 selective sweep signatures. All three specialists had more selective sweeps potentially resulting
604 from strong directional selection for adapting to new fitness peaks. However, while we might
605 expect more selective sweeps in *C. desquamator* genomes given the deeper valley on the fitness
606 landscape isolating the scale-eater phenotypes [10,12], C. *brontotheriodes* had the most selective
607 sweeps detected in their genome. They also have the longest sweeps detected (e.g. 100-kb),

608 suggesting that selection may have occurred most recently in the *C. brontotheriodes*. This
609 matches with the most recent divergence event being between generalist and *C. brontotheriodes*
610 in Osprey Lake. An intriguing implication of this result is the potentially long wait time for
611 speciation of *C. brontotheriodes* species compared *C. desquamator* despite the shallower fitness
612 valley isolating *brontotheroides* from generalists. However, we cannot yet rule out that the recent
613 divergence time estimated in Osprey Lake reflects a more recent arrival of *C. brontotheriodes* to
614 that lake after initially diverging long ago in another lake not incorporated in our demographic
615 model.

616

617 **Methods**

618 *Sampling*

619 The *C.* sp. 'wide-mouth' individuals were collected on San Salvador Island in the Bahamas
620 using hand and seine nets between 2017 and 2018. 'Wide-mouth' individuals were collected
621 from 5 lakes in which taxa occurs in sympatry with just *C. variegatus* (Great Lake, and Stout's
622 Lake) or with generalist and *C. desquamator* (Oyster Pond, Osprey Lake, and Mermaid's Pond,;
623 Fig. 1). In Oyster Pond and Little Lake, *C. desquamator* is extremely rare (only a single Oyster
624 Pond individual grouped genetically and morphologically with *C. desquamator*), so Osprey Lake
625 appears to be the only lake where all three species and the recently discovered 'wide-mouth'
626 coexist at appreciable frequencies in sympatry. 'Wide-mouth' individuals have also been
627 collected in Little Lake in the past (Bruce Turner, pers. obs. 1990s).

628 Fishes were euthanized in an overdose of buffered MS-222 (Finquel, Inc.) following
629 approved protocols from the University of North Carolina at Chapel Hill Animal Care and Use

630 Committee (#18-061.0), and the University of California, Berkeley Animal Care and Use
631 Committee (AUP-2015-01-7053) and preserved in 95-100% ethanol.
632
633 *Ecological and morphological characterization of 'wide-mouth' scale-eater*
634 Multiple individuals from 3 lake populations (Osprey Lake, Great Lake, and Oyster Pond) in
635 which we had measurable specimens of the species (n=84) were measured for 9 traits using dial
636 calipers. Traits were selected for specific connections to foraging performance [103,104] and that
637 differed across the three groups in a previous study when externally measured [10]. For each
638 specimen we measured (1) standard length from the anterior tip of the premaxilla to the posterior
639 margin on the midline of the caudal peduncle, (2) lower jaw length from the medial point of the
640 dentary on the lower jaw to the distal point of rotation on the quadrate-articular joint, (3) the
641 width of the buccal from the distance between the proximal sides of the buccal cavity in dorsal
642 view, (4) the height of the adductor mandibulae insertion from the vertex between the vertical
643 and horizontal arms of the preopercle to the dorsal margin of the hyomandibula, (5) the distance
644 from the insertion of the first ray of the dorsal fin to the insertion of the first ray of the anal fin,
645 (6) the height of the caudal peduncle from the dorsal and ventral procurrent rays on the caudal
646 fin, (7) neurocranium width from the narrowest distance between the eyes from the dorsal view,
647 (8) body width from just behind the posterior margins of each operculum in dorsal view, and (9)
648 diameter of the orbit. Measurements were made by a single observer (EJR). Repeatability of
649 measurements was assessed by remeasuring a random subset of 10 individuals per species twice.
650 Measurements on the full dataset were not taken until repeatability was above 85% per trait (r^2 in
651 a linear regression of both sets of measurements). To remove the effects of body size on trait
652 size, we used the residuals from a linear regression of the log-transformed trait on log

653 transformed standard length. We also compared these morphological measurements between lab-
654 reared F2 and wild caught specimens to rule out strong plasticity in traits of interest.
655 For a subset of individuals collected from each population (*C. variegatus, C.*
656 *desquamator,* and 'wide-mouth') in Osprey Lake, diet was characterized from stomach content
657 analyses (*n*=10 each) and stable isotope analyses (*n*=75; 42 *C. variegatus*, 16 *C. desquamator*, 17
658 'wide-mouth' individuals). These are two complementary approaches that reflect short-term and
659 long-term snapshots of the dietary differences among these groups. For stomach content analysis,
660 a single observer (EJR) dissected out a 1 cm portion of the gut from the posterior hindgut region
661 and counted the number of scales found. For stable isotope analyses, muscle tissue samples were
662 taken from the caudal peduncle region of each individual immediately after euthanasia in an
663 overdose of MS-222. Muscle samples were individually labeled and dried at 60° C for at least 24
664 hours. Foil-wrapped tissue samples were then sent to the UC Davis Stable isotope facility and
665 analyzed on a PDZ Europa ANCA-GSL elemental analyzer interfaced to a PDZ Europa 20-20
666 isotope ratio mass spectrometer to characterize the natural abundances of δ13C and δ15N among
667 individuals.
668
669 Genomic library preparation
670 We sequenced 24 'wide-mouth' individuals following protocols used in a previous study [105] in
671 which we sequenced genomes from *Cyprinodon variegatus*, *C. desquamator*, and *C.*
672 *bronototheroides*. Raw reads were mapped from these 24 individuals to a de-novo assembly of
673 *Cyprinodon brontotheroides* reference genome (v 1.0; total sequence length = 1,162,855,435 bp;
674 number of scaffolds = 15,698, scaffold N50 = 32 Mbp) with bwa-mem (v 0.7.12;[106]).
675 Duplicate reads were identified using MarkDuplicates and BAM indices were created using

676 BuildBamIndex in the Picard software package (http://picard.sourceforge.net(v.2.0.1)). We
677 followed the best practices guide recommended in the Genome Analysis Toolkit (v 3.5;[107]) to
678 call and refine our single nucleotide polymorphism (SNP) variant dataset using the program
679 HaplotypeCaller. Variants in 'wide-mouth' individuals were called jointly with the 202
680 individuals sequenced from a previous study [105]. We filtered SNPs based on the recommended
681 hard filter criteria (i.e. QD < 2.0; FS > 60; MQRankSum < -12.5; ReadPosRankSum < -
682 8;[107,108]) because we lacked high-quality known variants for these non-model species. After
683 selecting for only individuals from San Salvador Island, variants were additionally filtered to
684 remove SNPs with a minor allele frequency below 0.05, genotype quality below 20, or
685 containing more than 10% missing data across all individuals at the site using vcftools
686 (v.0.1.15;[109]). Variants in poorly mapped regions were then removed using a mask file
687 generated from the program SNPable (http://bit.ly/snpable; k-mer length =50, and
688 'stringency'=0.5). Our final dataset after filtering contained 6.4 million variants with 7.9x
689 median coverage per individual.
690
691 Testing for signatures of recent hybrids
692 We first tested whether these 'wide-mouth' individuals represented recent (e.g. F1/F2) hybrids of
693 *C. variegatus* and *C. desquamator* in the wild. These two young species do reproduce with each
694 other in the lab and rare hybrid spawning events have been observed in the wild (unpublished
695 data ME St. John). As a first visual assessment, we conducted principal component analysis on
696 *C. desquamator*, generalist, and 'wide-mouth' individuals to look for the genome-wide pattern
697 expected in PCAs in which recent hybrids between two populations are included. To perform the
698 PCA, the genetic dataset was first pruned for SNPs in strong linkage disequilibrium using the LD

699 pruning function (--indep-pairwise 50 5 0.5) in plink (v1.9;[110]), leaving 2.6 million variants.
700 We then ran a principal component analysis using the eigenvectors output by plink's pca
701 function (--pca). The first two principal components were plotted in R (R Core Team 2018
702 v3.5.0).

703 As a complementary assessment, we used an admixture model-based approach to
704 estimate the proportion of shared ancestry among individuals in our dataset using ADMIXTURE
705 (v.1.3.0)[111]. The number of populations (K) was decided upon using ADMIXTURE's cross-
706 validation method (--cv) across 1-10 population values of K. K = 4 was then chosen using the
707 broken-stick method. Ancestry proportions estimated by ADMIXTURE were plotted in R for the
708 K value with the highest likelihood and the two K values surrounding to explore whether the
709 strong signatures of population structure in Crescent Pond *C. desquamator* individuals was
710 masking hybridization signatures in any of the 'wide-mouth' populations.

711 Lastly, to discriminate among alternative evolutionary scenarios for the origin of 'wide-
712 mouth' and to estimate divergence time among all four species, we used demographic modeling
713 based on the folded minor allele frequency spectrum (mSFS). The observed mSFS was computed
714 using the SFStools script from D. Marques available on github
715 (https://github.com/marqueda/SFS-scripts). For these demographic model comparisons, we used
716 only individuals from Osprey Lake (*C. desquamator*: n=10; *C. variegatus* : n=12; *C.* sp. 'wide-
717 mouth': n=11; *C. brontotheriodes*: n=13) to avoid additional complex population structure across
718 ponds. We contrasted 28 demographic models of different topologies and gene flow scenarios
719 across the four groups (Fig S5;Table 1 and S2). For each model, the fit to the observed
720 multidimensional mSFS was maximized using the composite-likelihood method fastsimcoal
721 (v2.6.0.3;[69] with 100,000 coalescent simulations, 40 expectation-maximization cycles, and

722 pooling all entries with less than 20 SNPs). For parameter estimates, we used a wide search
723 range with log-uniform distributions with the range of some priors informed by previous
724 estimates of effective population size from MSMC and the age of the last glacial maximum
725 (~20kya) prior to which the lakes would have been dry on SSI. These ranges were not upper
726 bounded by these specified priors and so the simulations were free to explore parameter space
727 that exceeded the priors.

728 For each demographic model, we ran 100 independent *fastsimcoal2* runs to determine
729 the parameter estimates with the maximum likelihood. The best fitting demographic model was
730 identified using Akaike information criteria (AIC). To get confidence intervals for the parameter
731 estimates from the best fitting model, we simulated 100 mSFS based on the maximum likelihood
732 parameter estimates from our best fitting model and ran 50 independent runs with this model on
733 each simulated SFS. The parameter point estimates from the run with the highest likelihood (of
734 the 50 independent runs) from each simulated SFS were then used to compute 95 percentile
735 confidence intervals as a measure of uncertainty in the parameter estimates from the observed
736 SFS.

737

738 <u>Testing for shared adaptive alleles</u>

739 *Patterns of directional selection*

740 Various demographic histories can shift the distribution of low- and high-frequency derived
741 variants to falsely resemble signatures of hard selective sweeps. In a previous study, we used
742 MSMC analyses to infer histories of population size changes in *C. variegatus*, *C. desquamator*
743 and *C. brontotheriodes* (Richards et al. 2021). In this study, we repeated the same analysis for
744 the 'wide-mouth'. In order to account for demography of the 'wide-mouth' population in

745 downstream analyses, we used the MSMC (v. 1.0.1;[112] to infer historical effective population
746 size (N_e) changes in the 'wide-mouth'. We ran MSMC on unphased GATK-called genotypes
747 separately for a single individual 'wide-mouth' from Osprey Lake with 16x mean coverage
748 across its genome (Fig S4). As recommended in the MSMC documentation, we masked sites
749 with less than half or more than double the mean coverage for that individual or with a genotype
750 quality below 20. We also excluded sites with <10 reads as recommended by Nadachowska-
751 Brzyska et al. [113]. To scale the output of MSMC to real time and effective population sizes, we
752 used a one-year generation time [114] and the estimated spontaneous mutation rate of 1.56 $x10^{-8}$
753 estimated from high coverage sequencing of two independent pedigreed parent-offspring crosses
754 of San Salvador Island species from a previous study (Richards et al. 2021).
755 Across all four populations in Osprey Lake, we looked for regions that appeared to be
756 under strong divergent selection in the form of a hard selective sweep from the site frequency
757 spectrum using SweeD (v.3.3.4;[115]). In this calculation of the composite likelihood ratio
758 (CLR) of a sweep, we incorporated our empirical estimate of the decrease in population size for
759 each focal population estimated from MSMC analyses in 50-kb windows across scaffolds that
760 were at least 100-kb in length (99 scaffolds; 85.6% of the genome). We also calculated CLRs
761 across 100,000 scaffolds consisting of neutrally evolving sequences simulated with ms-move
762 [116], controlling for the impact of the inferred population size decreases over time for each
763 population from MSMC runs mentioned above (Fig. S4; Table S3). The CLR ratios for the
764 simulated datasets were then used to assess outlier CLR ratios from the empirical dataset.
765 Regions with CLR ratios above the 95th percentile value of CLR from the neutral simulated
766 dataset were considered candidate hard selective sweep regions (Table S3). We compared

767 selective sweeps across *C. variegatus, C. desquamator, C. brontotheriodes*, and 'wide-mouth' to
768 look for shared and unique selective sweeps among the four groups.
769
770 *Characterization of candidate adaptive alleles*
771 We searched for candidate adaptive alleles underlying divergent traits among the species by
772 overlapping selective sweeps regions with regions of high genetic divergence based on fixed or
773 nearly fixed SNPs between groups. We chose to look at nearly fixed SNPs over only fixed
774 variation to accommodate the ongoing geneflow occurring between these young species. We
775 took two approaches to finding fixed or nearly-fixed variants: 1) a fixed threshold of $F_{st} \geq 0.95$
776 across all comparisons and 2) and threshold of the 99.9th percentile of F_{st}, which varied among
777 comparisons (range of F_{st} 0.73-0.83).
778 We made the following pairwise comparisons for F_{st} calculations including a) between *C.*
779 *variegatus* and each of the specialists, b) each specialist against all other groups and c) shared
780 between two or three specialists against *C. variegatus*. For nearly fixed variants with the $F_{st} \geq$
781 0.95 threshold, we looked for putative function of the candidate adaptive alleles by looking at
782 gene annotations of any gene the variant was in or near (within 20-kb of the gene, which is
783 within the 50-kb LD decay estimate). We used available gene annotations from model organisms
784 of mice and zebrafish from MGI, ZFIN, and we checked other annotation databases and studies
785 for verification of putative function, including Phenoscape Knowledgebase
786 (https://kb.phenoscape.org/#/home), NCBI's PubMed (https://www.ncbi.nlm.nih.gov/pubmed),
787 and the Gene Ontology database using AMIGO2 [117] .
788 For the 99.9th percentile F_{st} variants: We performed gene ontology (GO) enrichment analyses
789 for genes near candidate adaptive variants using ShinyGo (v.0.51;[118]). In the *C.*

790 *brontotheroides* reference genome annotations (described in *de novo* genome assembly and
791 annotation section), gene symbols largely match human gene symbols. Thus, the best matching
792 species when we searched for enrichment across biological process ontologies curated mostly
793 human gene functions.
794
795 *Timing of selection on candidate adaptive alleles*
796 Lastly, we also determined the relative age of candidate adaptive alleles by generating estimates
797 of coalescent times using the R package starTMRCA (v0.6-1;[78]). For each candidate adaptive
798 allele that was unique to the three specialists and the 16 shared alleles between *C. desquamator*
799 and 'wide-mouth', a 1-Mb window surrounding the variant was extracted into separate vcfs for
800 individuals within each species. The program requires complete genotype data so we first filtered
801 out any individuals with more than 10% missing data (1 *C. brontotheriodes* and 2 'wide-mouth'
802 individuals). With Tassel5 [119], we then used the LD KKNI command to infer missing sites
803 based on LD for remaining individuals with less than 10% missing data. Subsequently we
804 removed the small number of sites with any missing data across individuals within each
805 population.
806 These sets of variants were then analyzed in starTMRCA with the mutation rate of
807 1.56×10^{-8} substitutions per base pair, and a recombination rate of 3.11×10^{-8} (from genome-wide
808 recombination estimate for stickleback; [120]). Each analysis was run three times per focal
809 adaptive allele and all runs were checked for convergence between and within runs. Most runs
810 rapidly converged within the initial 6000 steps, but 5 runs did not converge after an additional
811 4000 steps and were discarded from further analysis.
812

Acknowledgements

We thank Priya Moorjani, Michelle St. John, Joseph McGirr, Jacquelyn Galvez, David Tian, Austin Patton, and Joseph Heras for helpful comments on the manuscript; the Gerace Research Centre and Troy Day for logistical support; the governments of the Bahamas for permission to collect and export samples; the Vincent J. Coates Genomics Sequencing Center and Functional Genomics Laboratory at UC Berkeley for performing whole-genome library preparation and sequencing (supported by NIH S10 OD018174 Instrumentation Grant), and the University of California Berkeley for computational resources. This research was funded by the National Science Foundation DEB CAREER grant #1749764, National Institutes of Health grant 5R01DE027052-02, the University of North Carolina at Chapel Hill, and the University of California, Berkeley to CHM, and graduate research funding from the Museum of Vertebrate Zoology to EJR.

Author Contributions

Conceptualization: EJR,CHM; Data Collection: EJR,CHM; Statistical analyses: EJR; Resources: CHM; Visualization: EJR,CHM; Original draft: EJR; Revising: EJR, CHM

Declaration of Interests

The authors declare no competing interests.

References

1. Martin CH, Richards EJ. The Paradox behind the Pattern of Rapid Adaptive Radiation: How Can the Speciation Process Sustain Itself through an Early Burst? Annu Rev Ecol Evol Syst. 2019;

2. Dieckmann U, Doebeli M. On the origin of species by sympatric speciation. Nature. Macmillan Magazines Ltd.; 1999;400: 354. Available: http://dx.doi.org/10.1038/22521
3. Polechová J, Barton NH, Gavrilefs S. Speciation thrrough competition: a critical review. Evolution (N Y). The Society for the Study of Evolution; 2005;59: 1194–1210. doi:10.1554/04-691
4. Bolnick DI. Multi-species outcomes in a common model of sympatric speciation. J Theor Biol. 2006;241: 734–744. doi:10.1016/j.jtbi.2006.01.009
5. Ito HC, Dieckmann U. A new mechanism for recurrent adaptive radiations. Am Nat. 2007;170. doi:10.1086/521229
6. Kondrashov AS, Kondrashov FA. Interactions among quantitative traits in the course of sympatric speciation. Nature. Macmillan Magazines Ltd.; 1999;400: 351–354. Available: http://dx.doi.org/10.1038/22514
7. Gavrilets S. Models of speciation: where are we now? J Hered. 2014;105: 743–755. doi:10.1093/jhered/esu045
8. Gavrilets S. Fitness landscape and origin of species. Princeton, NJ: Princeton University Press; 2004.
9. Gavrilets S, Vose A. Dynamic patterns of adaptive radiation. Proc Natl Acad Sci U S A. 2005;102: 18040–18045. doi:10.1073/pnas.0506330102
10. Martin CH, Wainwright PC. Multiple fitness peaks on the adaptive landscape drive adaptive radiation in the wild. Science. 2013;339: 208–11. doi:10.1126/science.1227710
11. Martin CH. Context dependence in complex adaptive landscapes: frequency and trait-dependent selection surfaces within an adaptive radiation of Caribbean pupfishes. Evolution (N Y). 2016;70: 1265–1282. doi:10.1111/evo.12932
12. Martin CH, Gould KJ. Surprising spatiotemporal stability of a multi-peak fitness landscape revealed by independent field experiments measuring hybrid fitness. Evol Lett. 2020; 530–544. doi:10.1002/evl3.195
13. Patton AH, Richards EJ, Gould KJ, Buie LK, Christopher H. Adaptive introgression and de novo mutations increase access to novel fitness peaks on the fitness landscape during a vertebrate adaptive radiation Keywords : fitness landscape ; adaptive radiation ; introgression ; standing genetic variation ; de novo mutation Introduction First conceptualized by Sewell Wright in 1932 , the adaptive landscape describes the complex relationship between genotype or phenotype and fitness (1). The landscape is a concept , metaphor , and an empirical measurement that exerts substantial influence over all evolutionary dynamics (2 – 6). Fitness landscapes were originally depicted as high-dimensional networks spanning genotypic space in which each genotype is associated with fitness (1). Simpson (7) later described the phenotypic evolution of populations through time on a rugged landscape , in which isolated clusters of fitness peaks represent ‘ adaptive zones ’ to which populations evolve from adjacent regions of low fitness (8). Lande and Arnold formalized the analysis of selection and estimation of phenotypic fitness landscapes (9 – 11), leading to empirical studies of fitness landscapes in numerous empirical systems (12 – 18). Fitness surfaces also provide a central component of speciation models and theory (19 – 21). Populations may speciate through a process of divergent selection (22), either on static landscapes or negative frequency-dependent disruptive selection (23 – 28). A fundamental concept in fitness landscape theory is that not all genotypic trajectories are accessible (5 , 29 , 30); only those paths that monotonically increase in fitness at each mutational step are evolutionarily accessible , an

884 expectation stemming from Fisher ' s fundamental theorem (31). These accessible
885 genotypic trajectories can thus be considered potential adaptive walks under Fisher ' s
886 geometric model (31 , 32). Experimental studies of adaptive walks in nature are
887 increasingly common , including the evolution of toxin resistance in monarch butterflies (
888 33), metabolism and citrate exploitation in E . coli (34) (35), and host-shift. 2021;
889 14. Pfaender J, Hadiaty RK, Schliewen UK, Herder F. Rugged adaptive landscapes shape a
890 complex, sympatric radiation. Proc R Soc B Biol Sci. 2016;283: 11–13.
891 doi:10.1098/rspb.2015.2342
892 15. Arnegard ME, McGee MD, Matthews B, Marchinko KB, Conte GL, Kabir S, et al.
893 Genetics of ecological divergence during speciation. Nature. Nature Publishing Group, a
894 division of Macmillan Publishers Limited. All Rights Reserved.; 2014;511: 1–17.
895 doi:10.1038/nature13301
896 16. Bank C, Matuszewski S, Hietpas RT, Jensen JD. On the (un)predictability of a large
897 intragenic fitness landscape. Proc Natl Acad Sci U S A. 2016;113: 14085–14090.
898 doi:10.1073/pnas.1612676113
899 17. Wright S. The roles of mutation, inbreeding, crossbreeding and selection in evolution.
900 Proc Sixth Int Congr Genet. 1932;1: 356–366.
901 18. Burch CL, Chao L. Epistasis and its relationship to canalization in the RNA virus φ6.
902 Genetics. 2004;167: 559–567. doi:10.1534/genetics.103.021196
903 19. Arnold SJ, Pfrender ME, G. JA. The Apaptive Landscape as a conceptual bridge between
904 mico- and macroevolution. Genetica. 2001;112–113: 9–32.
905 20. Svennson E, Calsbeek R. The adaptive landscape in evolutionary biology. Oxford
906 University Press; 2012.
907 21. Calsbeek R, Irschick DJ. The quick and the dead: Correlational selection on morphology,
908 performance, and habitat use in island lizards. Evolution (N Y). 2007;61: 2493–2503.
909 doi:10.1111/j.1558-5646.2007.00206.x
910 22. Grant PR, Grant RB. How and Why Species Multiply. Princeton University Press; 2008.
911 23. Givnish TJ, Sytsma KJ, Smith J, Hahn W, DH B, Burkhardt E. Molecular evolution and
912 adaptive radiation in *Brocchinia* (Bromeliaceae: Pitcairnioideae) atop tepuis of the
913 Guyana Shield. Molecular evolution and adaptive radiation. Cambridge: Cambridge
914 University Press; 1997. pp. 259–311.
915 24. Givnish TJ, Burkhardt EL, Happel RE, Weintraub JD. Carnivory in the Bromeliad
916 Brocchinia reducta , with a Cost / Benefit Model for the General Restriction of
917 Carnivorous Plants to Sunny , Moist , Nutrient-Poor Habitats. Am Nat. 1984;124: 479–
918 497.
919 25. Goldschmidt R. Some Aspects of Evolution. Science (80-). American Association for the
920 Advancement of Science; 1933;78: 539–547. Available:
921 http://www.jstor.org/stable/1660832
922 26. Goldschmidt R. The material basis of evolution. Yale University Press; 1940.
923 27. Mayr E. The emergence of evolutionary novelties. Evol after Darwin. 1960;
924 28. Charlesworth B, Lande R, Slatkin M. A Neo-Darwinian Commentary on Macroevolution.
925 Evolution (N Y). [Society for the Study of Evolution, Wiley]; 1982;36: 474–498.
926 doi:10.2307/2408095
927 29. Simpson GG. The Major Features of Evolution [Internet]. Columbia University Press;
928 1953. doi:doi:10.7312/simp93764
929 30. Dobzhanksy T. Genetics and the origin of species. New York: Columbia University Press;

930 1937.
931 31. Rieseberg LH, Raymond O, Rosenthal DM, Lai Z, Livingstone K, Nakazato T, et al.
932 Major Ecological Transitions in Wild Sunflowers Facilitated by Hybridization. Science
933 (80-). 2003;301: 1211–1216. doi:10.1126/science.1086949
934 32. Gross BL, Rieseberg LH. The ecological genetics of homoploid hybrid speciation. J
935 Hered. 2005;96: 241–252. doi:10.1093/jhered/esi026
936 33. Moran BM, Payne C, Langdon Q, Powell DL, Brandvain Y, Schumer. The genomic
937 consequences of hybridization. 2020; Available: https://arxiv.org/pdf/2012.04077.pdf
938 34. Brice C, Zhang Z, Bendixsen D, Stelkens R. Hybridization Outcomes Have Strong
939 Genomic and Environmental Contingencies. Am Nat. 2021;198: E000–E000.
940 doi:10.1086/715356
941 35. Schumer M, Rosenthal GG, Andolfatto P. What do we mean when we talk about hybrid
942 speciation? Heredity (Edinb). 2018;120: 379–382. doi:10.1038/s41437-017-0036-z
943 36. Nieto Feliner G, Álvarez I, Fuertes-Aguilar J, Heuertz M, Marques I, Moharrek F, et al. Is
944 homoploid hybrid speciation that rare? An empiricist's view. Heredity (Edinb). 2017;118:
945 513–516. doi:10.1038/hdy.2017.7
946 37. Erwin DH. Prospects for a General Theory of Evolutionary Novelty. J Comput Biol.
947 2019;26: 735–744. doi:10.1089/cmb.2019.0089
948 38. Erwin DH. A conceptual framework of evolutionary novelty and innovation. Biol Rev.
949 2021;96: 1–15. doi:10.1111/brv.12643
950 39. Blount ZD, Barrick JE, Davidson CJ, Lenski RE. Genomic analysis of a key innovation in
951 an experimental *Escherichia coli* population. Nature. 2012;489: 513–518.
952 doi:10.1038/nature11514
953 40. Blount ZD, Maddamsetti R, Grant NA, Ahmed ST, Jagdish T, Baxter JA, et al. Genomic
954 and phenotypic evolution of escherichia coli in a novel citrate-only resource environment.
955 Elife. 2020;9: 1–64. doi:10.7554/eLife.55414
956 41. Turner C, Blount Z, Mitchell D, Lenski R. Evolution and coexistence in response to a key
957 innovation in a long-term evolution experiment with Escherichia coli. bioRxiv. 2015;
958 020958. doi:10.1101/020958
959 42. Quandt EM, Deatherage DE, Ellington AD, Georgiou G, Barrick JE. Recursive
960 genomewide recombination and sequencing reveals a key refinement step in the evolution
961 of a metabolic innovation in Escherichia coli. Proc Natl Acad Sci U S A. 2014;111: 2217–
962 2222. doi:10.1073/pnas.1314561111
963 43. Jagdish T, Morris JJ, Wade BD, Blount ZD. Probing the Deep Genetic Basis of a Novel
964 Trait in Escherichia coli* BT - Evolution in Action: Past, Present and Future: A
965 Festschrift in Honor of Erik D. Goodman. In: Banzhaf W, Cheng BHC, Deb K, Holekamp
966 KE, Lenski RE, Ofria C, et al., editors. Cham: Springer International Publishing; 2020. pp.
967 107–122. doi:10.1007/978-3-030-39831-6_10
968 44. Seehausen O. Hybridization and adaptive radiation. Trends Ecol Evol. 2004;19: 198–207.
969 doi:10.1016/j.tree.2004.01.003
970 45. Lotsy J. Species or Linneon. Genetica. 1925;7: 487–506.
971 46. Grant V. Plant Speciation. New York: Columbia University Press; 1981.
972 47. Meier JI, Stelkens RB, Joyce DA, Schliewen UK, Selz OM, Wagner CE, et al.
973 Hybridization explains rapid adaptive radiation in Lake Mweru cichlid fi shes. Nat
974 Commun. Springer US; 2019; doi:10.1038/s41467-019-13278-z
975 48. Meier JI, Marques DA, Mwaiko S, Wagner CE, Excoffier L, Seehausen O. Ancient

hybridization fuels rapid cichlid fish adaptive radiations. Nat Commun. Nature Publishing Group; 2017;8: 14363. doi:10.1038/ncomms14363

49. The Heliconius Genome Consortium, Dasmahapatra KK, Walters JR, Briscoe AD, Davey JW, Whibley A, et al. Butterfly genome reveals promiscuous exchange of mimicry adaptations among species. Nature. Nature Publishing Group; 2012;487: 94–98. doi:10.1038/nature11041
50. Lamichhaney S, Berglund J, Almén MS, Maqbool K, Grabherr M, Martinez-Barrio A, et al. Evolution of Darwin's finches and their beaks revealed by genome sequencing. Nature. 2015;518: 371–375. doi:10.1038/nature14181
51. Richards EJ, Martin CH. Adaptive introgression from distant Caribbean islands contributed to the diversification of a microendemic adaptive radiation of trophic specialist pupfishes. PLoS Genet. 2017;13: 1–35. doi:10.1371/journal.pgen.1006919
52. Poelstra JW, Richards EJ, Martin CH. Speciation in sympatry with ongoing secondary gene flow and a potential olfactory trigger in a radiation of Cameroon cichlids. Mol Ecol. 2018;27: 1–19. doi:10.1111/mec.14784
53. Richards EJ, Poelstra JW, Martin CH. Don't throw out the sympatric speciation with the crater lake water: fine-scale investigation of introgression provides equivocal support for causal role of secondary gene flow in one of the clearest examples of sympatric speciation. Evol Lett. 2018;2: 524–540. Available: https://onlinelibrary.wiley.com/doi/full/10.1002/evl3.78
54. Lamichhaney S, Berglund J, Almén MS, Maqbool K, Grabherr M, Martinez-Barrio A, et al. Evolution of Darwin's finches and their beaks revealed by genome sequencing. Nature. 2015;518: 371–375. doi:10.1038/nature14181
55. Jay P, Whibley A, Frézal L, Rodríguez de Cara MÁ, Nowell RW, Mallet J, et al. Supergene Evolution Triggered by the Introgression of a Chromosomal Inversion. Curr Biol. 2018;28: 1839-1845.e3. doi:https://doi.org/10.1016/j.cub.2018.04.072
56. Zhang W, Dasmahapatra KK, Mallet J, Moreira GRP, Kronforst MR. Genome-wide introgression among distantly related Heliconius butterfly species. Genome Biol. Genome Biology; 2016;17: 25. doi:10.1186/s13059-016-0889-0
57. Edelman NB, Frandsen PB, Miyagi M, Clavijo B, Davey J, Dikow RB, et al. Genomic architecture and introgression shape a butterfly radiation. Science (80-). 2019;366: 594 LP – 599. doi:10.1126/science.aaw2090
58. Stroud JT, Losos JB. Ecological Opportunity and Adaptive Radiation. Annu Rev Ecol Evol Syst. 2016;47: 507–532. doi:10.1146/annurev-ecolsys-121415-032254
59. Gavrilets S, Losos JB. Adaptive radiation: contrasting theory with data. Science. 2009;323: 732–7. doi:10.1126/science.1157966
60. Whittaker R. Evolution of species diversity in land communities. Evol Biol. 1977;
61. Martin CH, Wainwright PC. A remarkable species flock of *Cyprinodon* pupfishes endemic to San Salvador Island, Bahamas. Bull Peabody Museum Nat Hist. 2013;54: 231–240.
62. Turner BJ, Duvernell DD, Bunt TM, Barton MG. Reproductive isolation among endemic pupfishes (Cyprinodon) on San Salvador Island, Bahamas: Microsatellite evidence. Biol J Linn Soc. 2008;95: 566–582. doi:10.1111/j.1095-8312.2008.01079.x
63. Hagey FM, Mylroie J. Pleistocene lake and lagoon deposits, San Salvador Island, Bahamas. Geol Soc Am. 1995;30: 77–90.
64. Clark PU, Dyke AS, Shakun JD, Carlson AE, Clark J, Wohlfarth B, et al. The Last Glacial

1022 Maximum. Science (80-). 2009;325: 710–714. doi:10.1126/science.1172873
1023 65. Zamani N, Russell P, Lantz H, Hoeppner MP, Meadows JR, Vijay N, et al. Unsupervised
1024 genome-wide recognition of local relationship patterns. BMC Genomics. 2013;14: 347.
1025 doi:10.1186/1471-2164-14-347
1026 66. Martin CH, Gould K, Bocklage C. Surprising spatiotemporal stability and frequency-
1027 independence across multiple fitness peaks driving adaptive radiation in the wild. 2019;
1028 67. Martin CH, Wainwright PC. On the measurement of ecological novelty: scale-eating
1029 pupfish are separated by 168 my from other scale-eating fishes. PLoS One. 2013;8:
1030 e71164. doi:10.1371/journal.pone.0071164
1031 68. Richards EJ, McGirr JA, Wang JR, St. John ME, Poelstra JW, Solano MJ, et al. A
1032 vertebrate adaptive radiation is assembled from an ancient and disjunct spatiotemporal
1033 landscape. Proc Natl Acad Sci U S A. 2021;118. doi:10.1073/pnas.2011811118
1034 69. Excoffier L, Dupanloup I, Huerta-Sánchez E, Sousa VC, Foll M. Robust Demographic
1035 Inference from Genomic and SNP Data. PLOS Genet. Public Library of Science; 2013;9:
1036 e1003905. doi:10.1371/journal.pgen.1003905
1037 70. Mcgirr JA, Martin CH. Parallel evolution of gene expression between trophic specialists
1038 despite divergent genotypes and morphologies. Evol Lett. 2018;2: 62–75.
1039 doi:10.1002/evl3.41
1040 71. Dickinson ME, Flenniken AM, Ji X, Teboul L, Wong MD, White JK, et al. High-
1041 throughput discovery of novel developmental phenotypes. Nature. Nature Publishing
1042 Group; 2016;537: 508–514. doi:10.1038/nature19356
1043 72. Lee JY, Seo D, You J, Chung S, Park JS, Lee JH, et al. The deubiquitinating enzyme,
1044 ubiquitin-specific peptidase 50, regulates inflammasome activation by targeting the ASC
1045 adaptor protein. FEBS Lett. 2017;591: 479–490. doi:10.1002/1873-3468.12558
1046 73. Heras J, Martin C. Nonadaptive radiation of the gut microbiome in an adaptive radiation
1047 of Cyprinodon pupfishes with minor shifts for scale-eating. bioRxiv. Cold Spring Harbor
1048 Laboratory; 2021;
1049 74. Soupene E. ATP8A1 activity and phosphatidylserine transbilayer movement. J Receptor
1050 Ligand Channel Res. 2008;Volume 1: 1–10. doi:10.2147/jrlcr.s3773
1051 75. Thomas T, Voss AK, Chowdhury K, Gruss P. Querkopf, a MYST family histone
1052 acetyltransferase, is required for normal cerebral cortex development. Development.
1053 England; 2000;127: 2537–2548.
1054 76. Kraft M, Cirstea IC, Voss AK, Thomas T, Goehring I, Sheikh BN, et al. Disruption of the
1055 histone acetyltransferase MYST4 leads to a noonan syndrome-like phenotype and
1056 hyperactivated MAPK signaling in humans and mice. J Clin Invest. 2011;121: 3479–3491.
1057 doi:10.1172/JCI43428
1058 77. Clayton-Smith J, O'Sullivan J, Daly S, Bhaskar S, Day R, Anderson B, et al. Whole-
1059 exome-sequencing identifies mutations in histone acetyltransferase gene KAT6B in
1060 individuals with the say-barber-biesecker variant of Ohdo syndrome. Am J Hum Genet.
1061 The American Society of Human Genetics; 2011;89: 675–681.
1062 doi:10.1016/j.ajhg.2011.10.008
1063 78. Smith J, Coop G, Stephens M, Novembre J. Estimating Time to the Common Ancestor for
1064 a Beneficial Allele. Mol Biol Evol. 2018;35: 1003–1017. doi:10.1101/071241
1065 79. Hibbins MS, Hahn MW. Phylogenomic approaches to detecting and characterizing
1066 introgression. ecoevorxiv. 2021; doi:10.32942/osf.io/uahd8
1067 80. Rosenzweig BK, Pease JB, Besansky NJ, Hahn MW. Powerful methods for detecting

1068 introgressed regions from population genomic data. Mol Ecol. Wiley/Blackwell
1069 (10.1111); 2016;25: 2387–2397. doi:10.1111/mec.13610
1070 81. Geneva AJ, Muirhead CA, Kingan SB, Garrigan D. A New Method to Scan Genomes for
1071 Introgression in a Secondary Contact Model. PLoS One. Public Library of Science;
1072 2015;10: e0118621. Available: https://doi.org/10.1371/journal.pone.0118621
1073 82. Joly S, McLenachan PA, Lockhart PJ. A statistical approach for distinguishing
1074 hybridization and incomplete lineage sorting. Am Nat. 2009;174. doi:10.1086/600082
1075 83. Martin CH, Wainwright PC. Trophic novelty is linked to exceptional rates of
1076 morphological diversification in two adaptive radiations of cyprinodon pupfish. Evolution
1077 (N Y). 2011;65: 2197–2212. doi:10.1111/j.1558-5646.2011.01294.x
1078 84. Orr HA. The Population Genetics of Adaptation: The Distribution of Factors Fixed during
1079 Adaptive Evolution. Evolution (N Y). 1998;52: 935. doi:10.2307/2411226
1080 85. Orr HA. The genetic theory of adaptation: A brief history. Nat Rev Genet. 2005;6: 119–
1081 127. doi:10.1038/nrg1523
1082 86. Gillespie JH. Molecular Evolution Over the Mutational Landscape. Evolution (N Y).
1083 [Society for the Study of Evolution, Wiley]; 1984;38: 1116–1129. doi:10.2307/2408444
1084 87. Kauffman S, Levin S. Towards a general theory of adaptive walks on rugged landscapes. J
1085 Theor Biol. 1987;128: 11–45. doi:https://doi.org/10.1016/S0022-5193(87)80029-2
1086 88. Maynard Smith J. Natural Selection and the Concept of a Protein Space. Nature.
1087 1970;225: 563–564. doi:10.1038/225563a0
1088 89. Bell G. Evolutionary rescue and the limits of adaptation. Philos Trans R Soc B Biol Sci.
1089 Royal Society; 2013;368: 20120080. doi:10.1098/rstb.2012.0080
1090 90. Lindsey HA, Gallie J, Taylor S, Kerr B. Evolutionary rescue from extinction is contingent
1091 on a lower rate of environmental change. Nature. 2013;494: 463–467.
1092 doi:10.1038/nature11879
1093 91. Rousselle M, Simion P, Tilak M-K, Figuet E, Nabholz B, Galtier N. Is adaptation limited
1094 by mutation? A timescale-dependent effect of genetic diversity on the adaptive
1095 substitution rate in animals. PLOS Genet. Public Library of Science; 2020;16: e1008668.
1096 Available: https://doi.org/10.1371/journal.pgen.1008668
1097 92. Mani GS, Clarke BC. Mutational order: a major stochastic process in evolution. Proc R
1098 Soc London B Biol Sci. Royal Society; 1990;240: 29–37. doi:10.1098/rspb.1990.0025
1099 93. Schluter D. Evidence for Ecological Speciation and Its Alternative. Science (80-).
1100 2009;323: 737 LP – 741. doi:10.1126/science.1160006
1101 94. Good BH, McDonald MJ, Barrick JE, Lenski RE, Desai MM. The dynamics of molecular
1102 evolution over 60,000 generations. Nature. 2017;551: 45–50. doi:10.1038/nature24287
1103 95. Schluter D, Conte GL. Genetics and ecological speciation. Proc Natl Acad Sci. 2009;106:
1104 9955–9962. doi:10.1073/pnas.0901264106
1105 96. Patwa Z, Wahl LM. The fixation probability of beneficial mutations. J R Soc Interface.
1106 2008;5: 1279–1289. doi:10.1098/rsif.2008.0248
1107 97. Pavlidis P, Alachiotis N. A survey of methods and tools to detect recent and strong
1108 positive selection. J Biol Res. 2017;24: 7. doi:10.1186/s40709-017-0064-0
1109 98. Höllinger I, Pennings PS, Hermisson J. Polygenic adaptation: From sweeps to subtle
1110 frequency shifts. PLOS Genet. Public Library of Science; 2019;15: e1008035. Available:
1111 https://doi.org/10.1371/journal.pgen.1008035
1112 99. Barghi N, Hermisson J, Schlötterer C. Polygenic adaptation: a unifying framework to
1113 understand positive selection. Nat Rev Genet. Springer US; 2020;21: 769–781.

doi:10.1038/s41576-020-0250-z
100. Chevin LM, Hospital F. Selective sweep at a quantitative trait locus in the presence of background genetic variation. Genetics. 2008;180: 1645–1660. doi:10.1534/genetics.108.093351
101. Thornton KR. Polygenic adaptation to an environmental shift: Temporal dynamics of variation under Gaussian stabilizing selection and additive effects on a single trait. Genetics. 2019;213: 1513–1530. doi:10.1534/genetics.119.302662
102. Flint HJ, Scott KP, Louis P, Duncan SH. The role of the gut microbiota in nutrition and health. Nat Rev Gastroenterol Hepatol. 2012;9: 577–589. doi:10.1038/nrgastro.2012.156
103. Wainwright PC, Bellwood DR, Westneat MW, Grubich JR, Hoey AS. A functional morphospace for the skull of labrid fishes: Patterns of diversity in a complex biomechanical system. Biol J Linn Soc. 2004;82: 1–25. doi:10.1111/j.1095-8312.2004.00313.x
104. Patricia Hernandez L, Gibb AC, Ferry-Graham L. Trophic apparatus in cyprinodontiform fishes: Functional specializations for picking and scraping behaviors. J Morphol. 2009;270: 645–661. doi:10.1002/jmor.10711
105. Richards E, McGirr J, Wang J, St. John M, Poelstra J, Solano M, et al. Major stages of vertebrate adaptive radiation are assembled from a disparate spatiotemporal landscape. 2020; doi:10.1101/2020.03.12.988774
106. Li H, Durbin R. Inference of human population history from individual whole-genome sequences. Nature. Nature Publishing Group; 2011;475: 493–496. doi:10.1038/nature10231
107. DePristo MA, Banks E, Poplin R, Garimella K V, Maguire JR, Hartl C, et al. A framework for variation discovery and genotyping using next-generation DNA sequencing data. Nat Genet. 2011;43: 491–8. doi:10.1038/ng.806
108. Marsden CD, Lee Y, Kreppel K, Weakley A, Cornel A, Ferguson HM, et al. Diversity, differentiation, and linkage disequilibrium: prospects for association mapping in the malaria vector Anopheles arabiensis. G3 (Bethesda). 2014;4: 121–31. doi:10.1534/g3.113.008326
109. Danecek P, Auton A, Abecasis G, Albers CA, Banks E, DePristo MA, et al. The variant call format and VCFtools. Bioinformatics. 2011;27: 2156–2158. doi:10.1093/bioinformatics/btr330
110. Purcell S, Neale B, Todd-Brown K, Thomas L, Ferreira MAR, Bender D, et al. PLINK: A Tool Set for Whole-Genome Association and Population-Based Linkage Analyses. Am J Hum Genet. 2007;81: 559–575. doi:10.1086/519795
111. Alexander DH, Novembre J, Lange K. Fast model-based estimation of ancestry in unrelated individuals. Genome Res. Cold Spring Harbor Lab; 2009;19: 1655–1664.
112. Schiffels S, Durbin R. Inferring human population size and separation history from multiple genome sequences. Nat Genet. Nature Publishing Group, a division of Macmillan Publishers Limited. All Rights Reserved.; 2014;46: 919. doi:10.1038/ng.3015
113. Nadachowska-Brzyska K, Burri R, Smeds L, Ellegren H. PSMC analysis of effective population sizes in molecular ecology and its application to black-and-white Ficedula flycatchers. Mol Ecol. 2016;25: 1058–1072. doi:10.1111/mec.13540
114. Martin CH, Crawford JE, Turner BJ, Simons LH. Diabolical survival in Death Valley: recent pupfish colonization, gene flow and genetic assimilation in the smallest species range on earth. Proc R Soc B Biol Sci. 2016;283: 20152334. doi:10.1098/rspb.2015.2334

115. Pavlidis P, Živković D, Stamatakis A, Alachiotis N. SweeD: Likelihood-based detection of selective sweeps in thousands of genomes. Mol Biol Evol. 2013;30: 2224–2234. doi:10.1093/molbev/mst112
116. Garrigan D, Geneva A. msmove: A modified version of Hudson's coalescent simulator ms allowing for finer control and tracking of migrant genealogies. 2014. doi:10.6084/m9.figshare.1060474
117. Balsa-Canto E, Henriques D, Gabor A, Banga JR. AMIGO2, a toolbox for dynamic modeling, optimization and control in systems biology. Bioinformatics. 2016;32: 1–2. doi:10.1093/bioinformatics/btw411
118. Ge SX, Jung D. ShinyGO: a graphical enrichment tool for animals and plants. bioRxiv. 2018; 2. doi:10.1101/315150
119. Bradbury PJ, Zhang Z, Kroon DE, Casstevens TM, Ramdoss Y, Buckler ES. TASSEL: Software for association mapping of complex traits in diverse samples. Bioinformatics. 2007;23: 2633–2635. doi:10.1093/bioinformatics/btm308
120. Roesti M, Moser D, Berner D. Recombination in the threespine stickleback genome - Patterns and consequences. Mol Ecol. 2013;22: 3014–3027. doi:10.1111/mec.12322

Supplemental Figures and Tables:

We get by with a little help from our friends: diversity begets diversity through shared adaptive genetic variation

Emilie J. Richards[1,2] and Christopher H. Martin[1,2]

[1]Department of Integrative Biology, University of California, Berkeley

[2]Museum of Vertebrate Zoology, University of California, Berkeley

Correspondence: *chmartin@berkeley.edu*

Keywords: ecological speciation, ecomorph, adaptive radiation, novelty, innovation, selective sweep

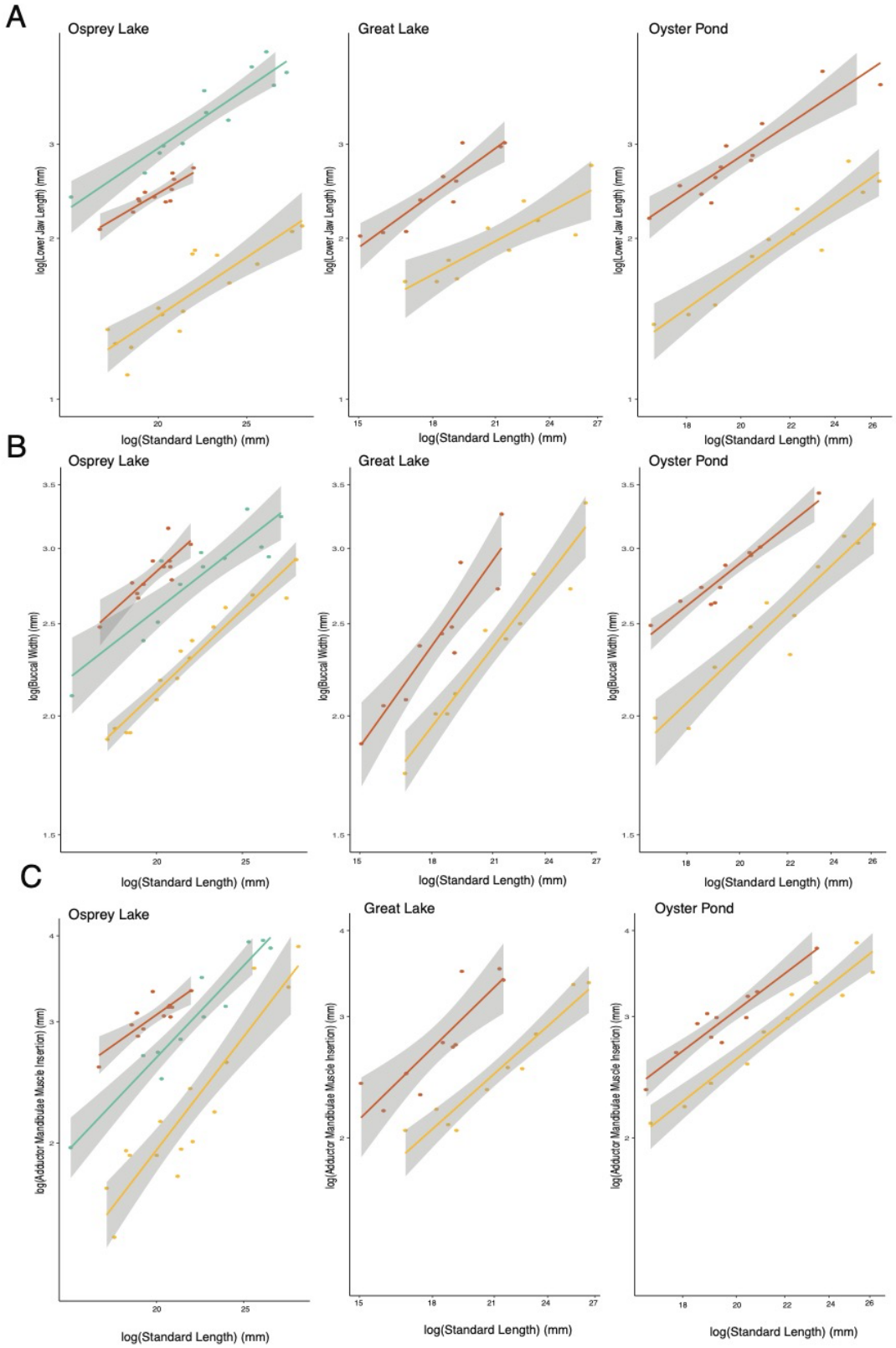
A
Osprey Lake
Great Lake
Oyster Pond
log(Lower Jaw Length) (mm)
log(Standard Length) (mm)
B
log(Buccal Width) (mm)
C
log(Adductor Mandibulae Muscle Insertion) (mm)

1196

1197

Figure S1. Relationships between three divergent traits and standard length across ponds. The relationship between standard length (mm) of individuals and their D) lower jaw length, E) buccal cavity width, and F) adductor mandibulae muscle insertion height across individuals the three species *C. desquamator* (teal), *C. variegatus* (gold), and *C.* sp. 'wide-mouth' (red-orange) across different ponds (Osprey, Oyster, and Great Lake). Colored lines represent linear model of these relationships for each species with their 95% confidence bands in gray.

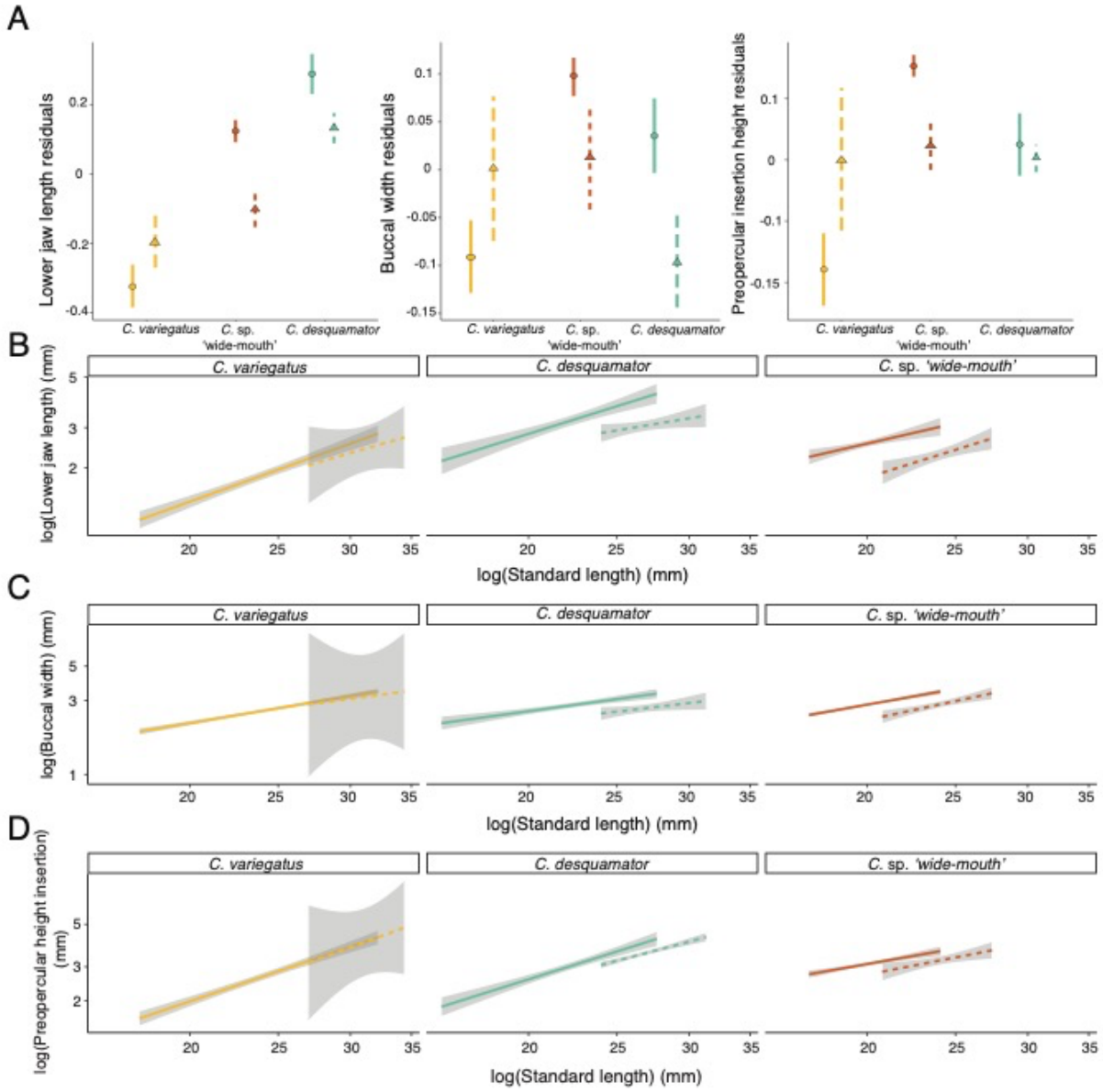

1206

1207 Figure S2. Comparison of the three focal divergent traits in lab and wild populations. A. 95% CI
1208 of the standardized sizes of lower jaw length (left), buccal width (center) and preopercular
1209 insertion height (right) for *C. variegatus* (gold), *C.* sp. 'wide-mouth' (red-orange) and *C.*
1210 *desquamator* (teal). Lines (wild: solid; lab:dashed) are the 95% CI interval and symbols (wild:
1211 circle; lab: triangle) represent the mean values of traits from each population. Lab raised
1212 individuals include F1 and F2 generations.
1213

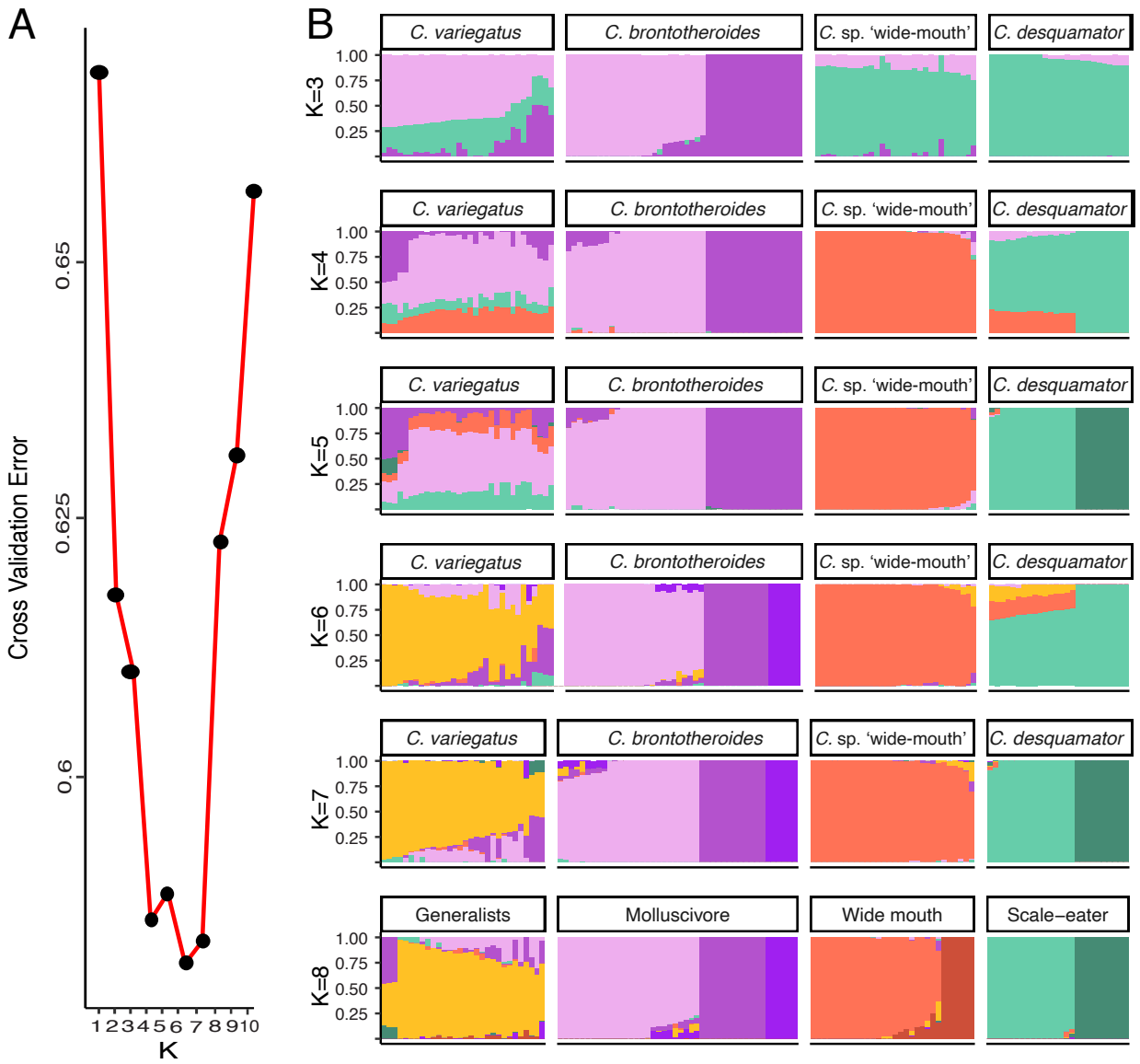

Figure S3. *C.* sp. 'wide-mouth' is not an admixed population. ADMIXTURE analysis of San Salvador Island populations using an LD-pruned subset of genetic variants from 109 individuals (78,840 variants). A) Cross validation error estimates from ADMIXTURE that indicate a K model of 6-7 were the best fit. B) Ancestry proportions across individuals of the three focal groups. Proportions were inferred from ADMIXTURE analyses with 2 values of K with the highest likelihood on the same LD-pruned dataset in A.

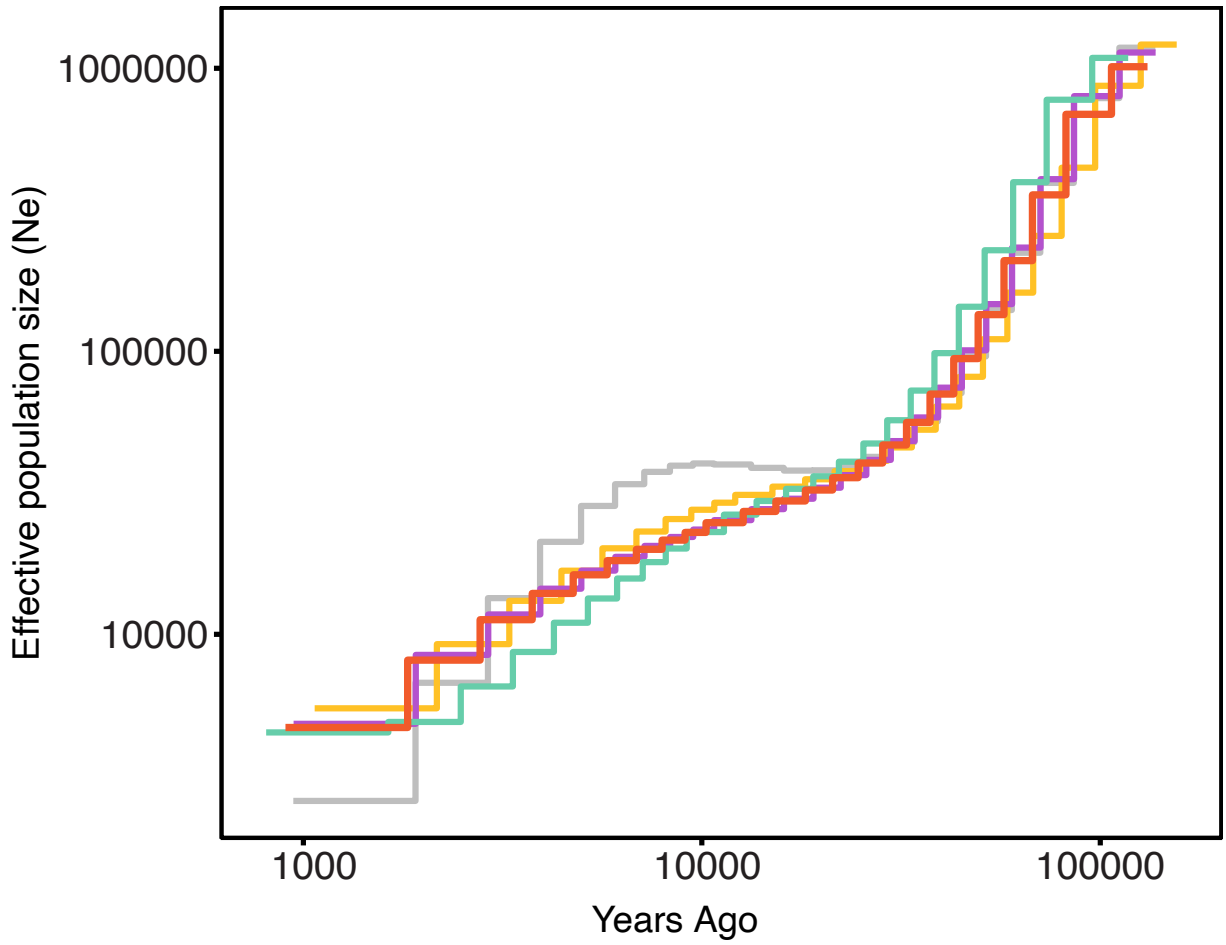

Fig S4. Changes in effective population size over time for Osprey populations inferred using MSMC [112] on high-coverage (18-36X) genomes from single individuals of each of the four species in Osprey Lake, San Salvador Island Bahamas: *C. variegatus* (gold), *C. brontotheroides* (purple), *C. desquamator* (teal), and C. sp. 'wide-mouth' (red-orange). Time was scaled using a mutation rate of 1.56x10-8 mutations/basepair/generation and a generation time of 1 year.

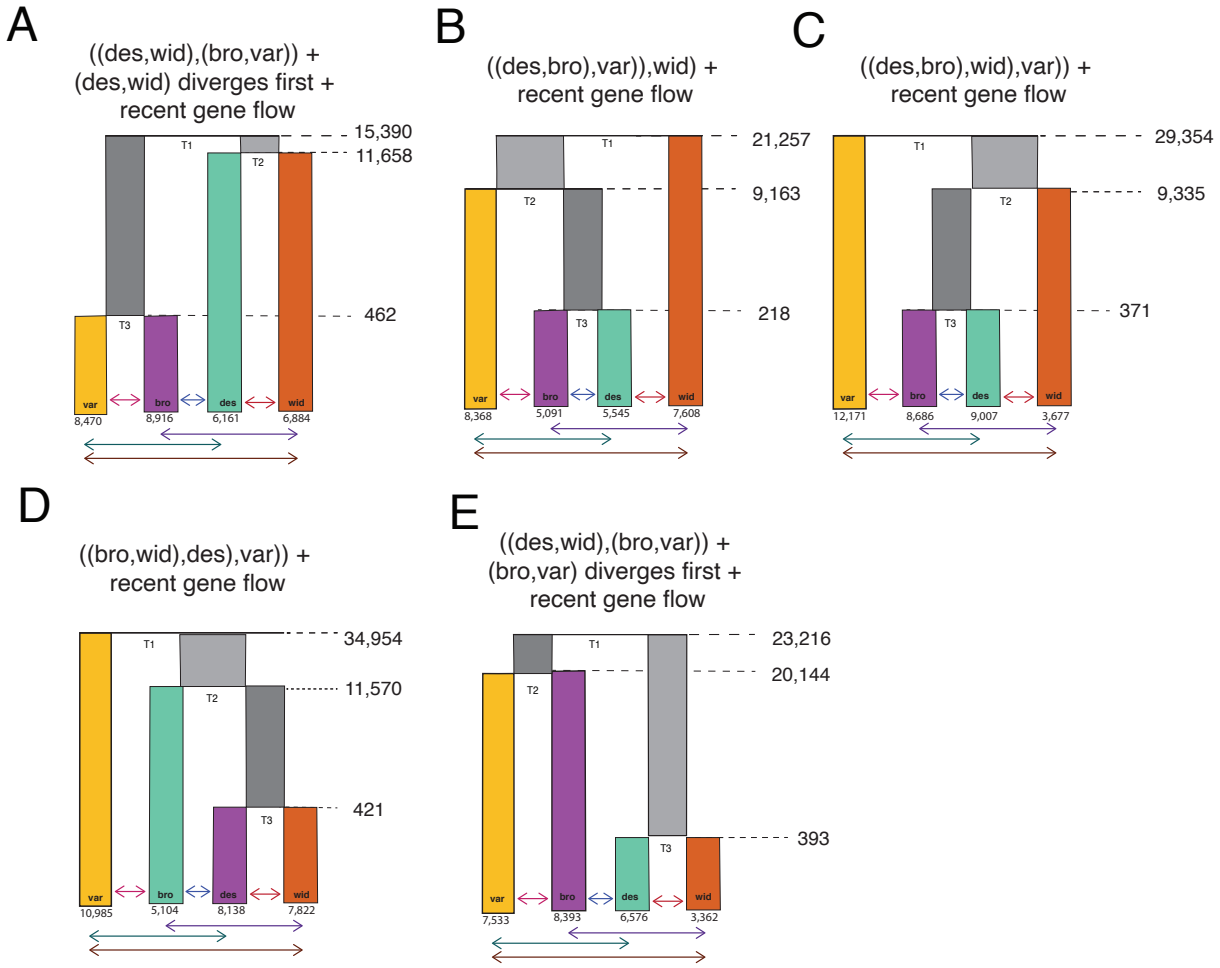

Fig S5. Top five best fitting demographic models for Osprey Lake. From a genetic dataset that was LD-pruned and had no missing information across individuals comprised of 67,400 SNPs. Listed in order of lowest AIC scores (Table 1 and S2) with best supported model in A. All top models were of recent bidirectional gene flow but varied in topology among the four species.

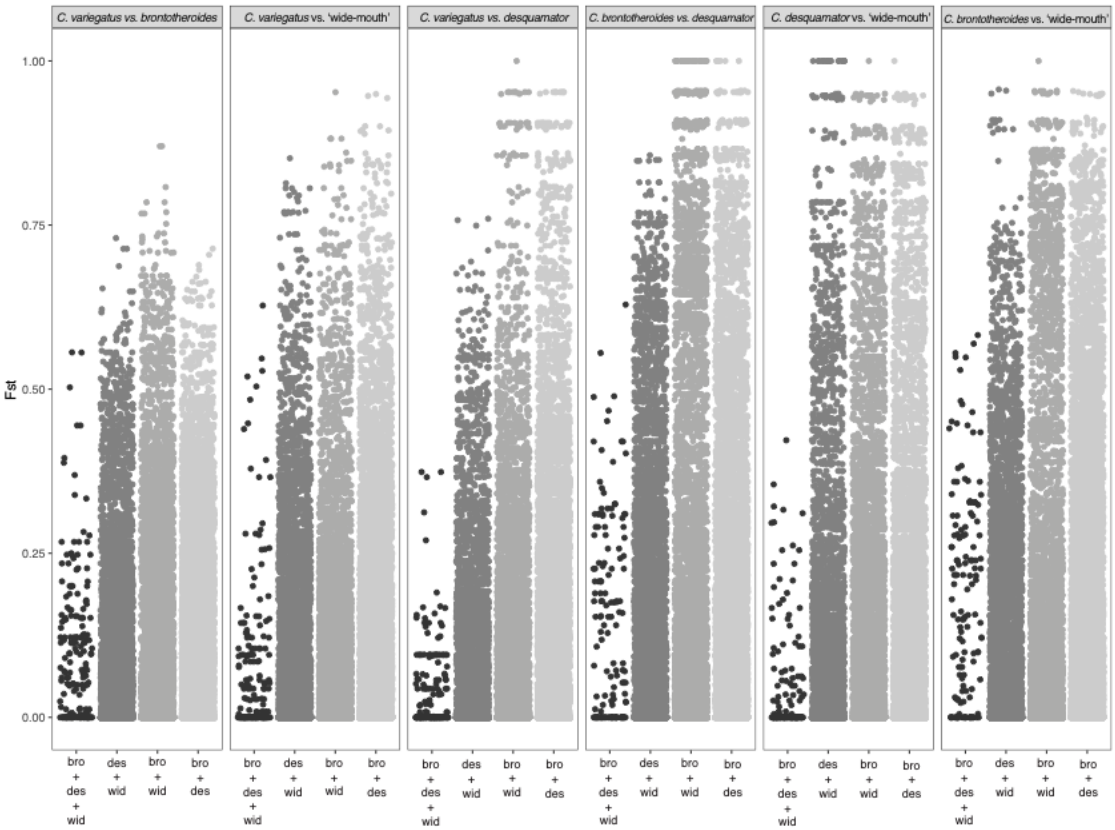

Fig S6. Genetic divergence among populations in Osprey Lake in regions of shared selection across two or more specialists. Each panel represents pairwise F_{st} comparison between two populations for every SNP found in regions under shared selection across two or more specialist species on San Salvador Island: C. brontotheroides (bro); C. desquamator (des), C. sp. 'wide-mouth' (wid). Regions shared across all three specialists (bro+des+wid) do not contain highly divergent SNPs between any of the species in the radiation. Highly divergent SNPs (Fst > 0.75) are only found in regions shared between one or two specialists.

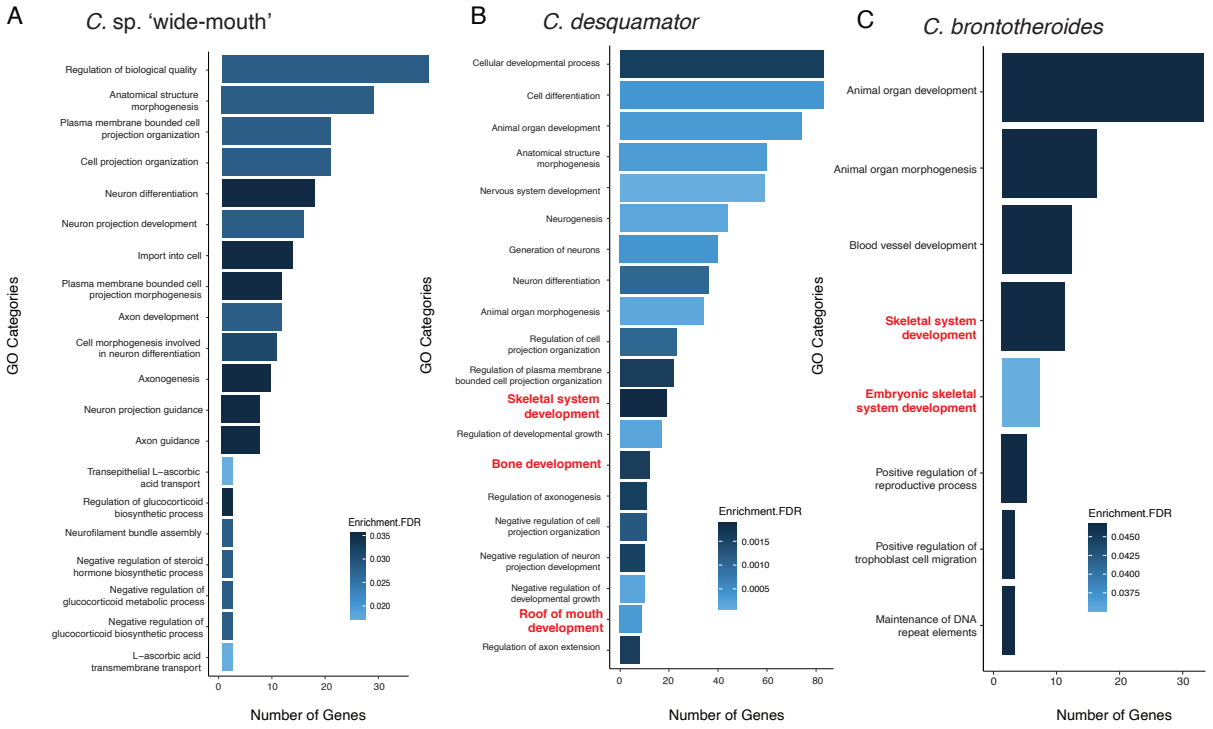

Fig S7. Top 20 enriched GO categories for divergent alleles in each of the three specialists. GO enrichment analyses were performed on genes in or near (within 20-kb) of a SNP that was under a hard selective sweep and strongly diverged from generalist species (top 1% of Fst values across genome) for a) 'wide-mouth' b) *C. desquamator*, and C) *C. brontotheriodes*. GO categories that were significantly enriched for relevant terms corresponding to craniofacial development, the major axes of morphological divergence in this radiation, are highlighted in red. All terms included were significant at an FDR < 0.05 and full list of terms in Data S1-3.

Table S1. No significant genome-wide signature of admixture among populations on San Salvador Islands. Results from three formal tests for introgression to assess whether 'wide-mouth' populations are hybrids between generalist *C. variegatus* and scale-eater *C. desquamator*: D-, f_3- and f_4-statistics across all possible combinations of Osprey Lake populations of generalist species. Significant f_3-statistic had Z-scores > -2; significant f_4 and D-statistic Z-scores were smaller than -2 and greater than 2. The only significant signature of admixture (bolded Z-scores) comes from D- and f_4-statistics based on relationships that violate the expected tree (((C. desquamator; 'wide-mouth'),Generalist),Outgroup) and therefore should not be interpreted as evidence of 'wide-mouth' being an admixed population. *C. variegatus* population from Rum Cay, the nearest neighbor island in the Bahamas to San Salvador Island was used as an outgroup population for D- and f_4-statistics.

f_3-statistic						
A	B	C	--	f_3	stderr	*Z*
C. variegatus	*C. desquamator*	C. sp. 'wide-mouth'		0.004626	0.00088	5.257
f_4- statistic						
P1	P2	P3	P4	f_4	stderr	*Z*
C. sp 'wide-mouth'	*C. desquamator*	*C. variegatus*	Rum Cay	-0.000196	0.000164	-1.2
C. sp 'wide-mouth'	*C. variegatus*	*C. desquamator*	Rum Cay	0.003971	0.000268	**14.836**
C. sp 'wide-mouth'	*C. variegatus*	*C. brontotheroides*	Rum Cay	0.000186	0.000201	0.927
D-statistic						
P1	P2	P3	Outgroup	D	stderr	*Z*
C.sp.'wide-mouth'	*C. desquamator*	*C. variegatus*	Rum Cay	-0.0018	0.001498	-1.199
C. sp. 'wide-mouth'	*C. variegatus*	*C. desquamator*	Rum Cay	0.035	0.002326	**15.068**
C. sp. 'wide-mouth'	*C. variegatus*	*C. brontotheroides*	Rum Cay	0.0017	0.001792	0.931

1316
1317 **Table S2. Support for the 28 demographic models for the evolution of the 'wide-mouths' from**
1318 **the site frequency spectrum.** The likelihood and AIC scores all demographic models estimated
1319 in *fastsimcoal2* for the Osprey populations of *C. variegatus* var), *C. brontotheroides* (bro), *C.*
1320 *desquamator* (des), and *C.* sp. 'wide-mouth' (wid) are presented here with a complete list of all
1321 models tested reported in Table S2. Change in likelihood (ΔLnL) represents the difference in
1322 likelihood from that of a simulated SFS expected by the demographic model tested. Change in
1323 AIC (ΔAIC) represents the difference in AIC scores from that of the model with the smallest
1324 ΔLnL. All models presented here represent different divergence scenarios with recent gene flow
1325 allowed, which had better support from the data than models with no gene flow or early gene
1326 flow. Visual representations of the top five models are depicted in Figure S5.
1327
1328

Divergence Model	LnL	ΔLnL	AIC	ΔAIC
(1) ((des,wid),(bro,var)) + (des,wid) diverges first + recent gene flow	-11701	1077	54133	0
(2) ((des,bro),var)) ,wid)) + recent gene flow	-11780	1112	54296	35
(3) ((des,bro),wid),var)) + recent gene flow	-11806	1138	54418	61
(4) ((bro,wid),des),var)) + recent gene flow	-11808	1140	54423	63
(5) ((des,wid),(bro,var)) + (bro,var) diverges first + recent gene flow	-11846	1178	54602	101
(6) ((des,wid), bro),var)) + recent gene flow	-11855	1187	54642	110
(7) ((des,bro),var)) ,wid))+ early gene flow	-12016	1348	55364	271
(8) ((des,var),bro), wid)) + recent gene flow	-12024	1356	55426	279
(9) ((wid,bro),des),var)) + early gene flow	-12086	1418	55688	341
(10) ((wid,des),bro),var)) + early gene flow	-11855	1419	55692	342
(11) ((des,wid),(bro,var)) + early gene flow	-12139	1471	55929	394
(12) ((des,wid), bro),var)) + no gene flow	-12315	1648	56738	570
(13) ((wid,bro),des),var)) + no gene flow	-12326	1658	56787	581
(14) ((des,bro),var)) ,wid))+ no gene flow	-12334	1667	56826	589
(15) ((des,wid),(bro,var)) + recent sister gene flow only	-12394	1726	57106	649
(16) ((des,wid),(bro,var))+ no gene flow	-12396	1728	57109	651
(17) ((wid,var)),bro),des)) + recent gene flow	-12399	1731	57148	654
(18) ((bro,var)) ,wid),des)) + recent gene flow	-12401	1733	57157	656
(19) ((wid,bro),var)),des)) + recent gene flow	-12401	1734	57163	657
(20) ((des,wid),var),bro)) + recent gene flow	-12420	1752	57244	675
(21) ((wid,var)),des),bro)) + recent gene flow	-12425	1757	57265	680
(22) ((des,var),wid),bro)) + recent gene flow	-12425	1757	57267	680
(23) ((wid,var)),(bro,des)) + no gene flow	-23245	12577	107070	11500
(24) ((wid,var)),(bro,des)) + early gene flow	-23658	12990	108976	11913
(25) ((wid,var)),(bro,des)) + recent gene flow	-23659	12991	109003	11914

(26) ((des,var),(bro,wid)) + early gene flow	-34983	24315	161129	23238
(27) ((des,var),(bro,wid)) + no gene flow	-34983	24315	161125	23238
(28) ((des,var),(bro,wid)) + recent gene flow	-34983	24315	161149	23238

Table S3. Parameters for selective sweep analyses in SweeD.
The 95th percentile of composite likelihood ratio threshold based on neutral simulations under the demographic scenario of decreasing population size through time inferred with MSMC (Fig S4), and the population size change and haplotype number information parameters required by SweeD for each species.

Species	CLR threshold	SweeD Commands
C. variegatus	0.40320	-folded -strictPolymorphic -G 0.407 -eN 5.45 181.8 -s 24
C. brontotheroides	0.43473	-folded -strictPolymorphic -G 0.389 -eN 5.88 196 -s 32
C. desquamator	0.40537	-folded -strictPolymorphic -G 0.218 -eN 8.11 270 -s 16
C. sp. 'wide-mouth'	0.39262	-folded -strictPolymorphic -G 0.203 -eN 8.57 276 -s 22

Table S4. Genetic divergence among the four populations in Osprey Lake, San Salvador Island across different thresholds of F_{st}. Relative measure of genetic divergence was calculated in pairwise combinations of the different species as the number of fixed SNPs between them, the number of fixed or nearly fixed SNPs between them, the top 1% of F_{st} between them from the distribution of F_{st} between SNPs and the genome-wide average F_{st} across all SNPs in the genome.

F_{st} Comparison	Number of fixed SNPs (F_{st} =1)	Number of nearly fixed SNPS ($F_{st} \geq$ 0.95)	Top 1%	Genome-wide average
C. sp. 'wide-mouth' vs *C. desquamator*	5,212	5,915	0.84	0.131
C. sp. 'wide-mouth' vs *C. brontotheroides*	5238	14,602	0.85	0.15
C. sp. 'wide-mouth' vs *C. variegatus*	247	869	0.68	0.104
C. desquamator vs *C. brontotheroides*	6941	22,088	0.86	0.17
C. desquamator vs *C. variegatus*	414	1,964	0.71	0.116
C. variegatus vs *C. brontotheroides*	110	567	0.637	0.09

1346 **Table S5. Comparison of the average absolute genetic divergence (D_{xy}) between the four**
1347 **species in Osprey Lake 'wide-mouth', *C. variegatus, C. desquamator and C. brontotheriodes***
1348 **and the shared adaptive alleles between scale-eater populations.**
1349

Comparison	Mean D_{xy}
C. variegatus vs *C. brontotheroides*	0.167
C. variegatus vs *C. desquamator*	0.169
C. variegatus vs *C.* sp. 'wide-mouth'	0.165
C. brontotheroides vs *C. desquamator*	0.162
C. brontotheroides vs *C.* sp. 'wide-mouth'	0.156
C. desquamator vs *C.* sp. 'wide-mouth'	0.157
Selective sweeps in *C.* sp. 'wide-mouth'	0.123
Shared genetic variants with *C. desquamator*	0.0814
Unique genetic variants in *C.* sp. 'wide-mouth'	0.24

1350
1351
1352
1353
1354

Table S7. The distribution of shared adaptive alleles between the two scale-eating species across the Caribbean. Numbers represent the copies of the *C. desquamator* and 'wide-mouth' allele present in outgroup populations collected from San Salvador Island (SS), Rum Cay (RC), Cat Island (CT), Exumas Islands (EX), Long Island (LG), Mayaguana (MG), New Providence Island (NPI) in the Bahamas. Lagunas Bavaros (BAV) and Etang Saumautre (ETA) in Dominican Republic, Sarasota Estuary in Florida (FL), Curacoa (CUR), Caicos Island (CAI) and Isla Margarita (MAR) in Venezuela.

			C. variegatus								*C. laciniatus*	*C. higuey*	*C. bondi*	*C. dearborni*		
Allele	Gene	Distribution	SS	RC	CT	EX	LG	MG	FL	NC	NPI	BAV	ETA	CUR	CAI	MAR
HiC_scaffold_6:907101	NA	SGV	0	0	1	0	0	0	0	12	0	0	0	0	0	0
HiC_scaffold_6:907425	NA	SGV	1	0	0	0	0	0	0	7	0	0	0	0	0	0
HiC_scaffold_6:907665	NA	SGV	0	0	0	0	0	0	0	7	0	0	0	0	0	0
HiC_scaffold_6:908229	NA	SGV	1	0	1	0	0	0	0	6	3	0	0	0	0	0
HiC_scaffold_6:908889	NA	SGV	1	0	0	0	0	0	0	6	0	0	0	0	0	0
HiC_scaffold_6:923182	NA	SGV	0	5	0	1	0	0	1	0	0	0	0	0	0	0
HiC_scaffold_6:923590	NA	SGV	0	5	0	2	0	0	0	0	0	0	0	0	0	0
HiC_scaffold_6:924203	NA	de novo	0	0	0	0	0	0	0	0	0	0	0	0	0	0
HiC_scaffold_6:929621	NA	SGV	1	2	1	0	0	0	0	0	0	0	0	0	0	0
HiC_scaffold_9:31763392	daam2	SGV	6	3	0	1	0	1	1	1	6	1	0	0	0	0
HiC_scaffold_9:31763400	daam2	SGV	8	5	0	1	1	0	1	8	10	8	0	0	0	0
HiC_scaffold_24:5390450	usp50	SGV	1	1	0	0	0	0	0	0	1	0	0	0	1	0
HiC_scaffold_43:27385265	NA	SGV	3	1	0	2	1	1	0	5	1	0	1	2	0	11
HiC_scaffold_43:27389200	NA	SGV	5	1	0	0	1	1	1	12	12	2	1	3	1	12
HiC_scaffold_44:14963656	atp8a1	SGV	3	1	0	1	0	1	1	12	12	2	1	3	1	12
HiC_scaffold_60:1798737	znf214	SGV	3	0	0	0	0	1	0	0	2	0	0	0	0	0